


Tectonic, magmatic, and metallogenic evolution of the Late Cretaceous arc in the Carpathian-Balkan orogen

Journal Article

Author(s):

Gallhofer, Daniela; von Quadt, Albrecht; Peytcheva, Irena; Schmid, Stefan M.; [Heinrich, Christoph A.](#) 

Publication date:

2015-09

Permanent link:

<https://doi.org/10.3929/ethz-b-000104227>

Rights / license:

[In Copyright - Non-Commercial Use Permitted](#)

Originally published in:

Tectonics 34(9), <https://doi.org/10.1002/2015TC003834>

Funding acknowledgement:

146681 - Fluid chemistry and fluid-rock interaction of Alpine veins, Central Alps (SNF)

146651 - Mineral resources: Physical dynamics driving chemical enrichment of rare metals (SNF)

This is the Green Open Access version of: Gallhofer, D., von Quadt, A., Peytcheva, I., Schmid, S. M., Heinrich, C. A., 2015. Tectonic, magmatic, and metallogenic evolution of the Late Cretaceous arc in the Carpathian-Balkan orogeny. *Tectonics*, vol. 34, pp. 1813-1836.
<https://doi.org/10.1002/2015TC003834>

Tectonic, magmatic, and metallogenic evolution of the Late Cretaceous arc in the Carpathian-Balkan orogeny

Daniela Gallhofer^a, Albrecht von Quadt^a, Irena Peytcheva^{a, b}, Stefan M. Schmid^c and Christoph A. Heinrich^{a, d}

^a Institute of Geochemistry and Petrology, ETH Zürich, Zürich, Switzerland.

^b Geological Institute, BAS, Sofia, Bulgaria.

^c Institute of Geophysics, ETH Zürich, Zürich, Switzerland.

^d Faculty of Mathematics and Natural Sciences, University of Zurich, Switzerland

Corresponding author: Daniela Gallhofer, Institute of Geochemistry and Petrology, ETH Zürich, 8092 Zürich, Switzerland (daniela.gallhofer@erdw.ethz.ch).

Key points:

- Major magmatic arc concealed by postsubduction continental collision
- Europe's active margin reconstructed using magma chemistry and geochronology
- Distribution of magmatic-hydrothermal ore deposits controlled by stress state

Abstract

The Apuseni-Banat-Timok-Srednogie Late Cretaceous magmatic arc in the Carpathian-Balkan orogen formed on the European margin during closure of the Neotethys Ocean. It was subsequently deformed into a complex orocline by continental collisions. The Cu-Au mineralized arc consists of geologically distinct segments: the Apuseni, Banat, Timok, Panagyurishte, and Eastern Srednogie segments. New U-Pb zircon ages and geochemical whole rock data for the Banat and Apuseni segments are combined with previously published data to reconstruct the original arc geometry and better constrain its tectonic evolution. Trace element and isotopic signatures of the arc magmas indicate a subduction-enriched source in all segments and variable contamination by continental crust. The magmatic arc was active for 25 Myr (~92–67 Ma). Across-arc age trends of progressively younger ages toward the inferred paleo-trench indicate gradual steepening of the subducting slab away from the upper plate European margin. This leads to asthenospheric corner flow in the overriding plate, which is recorded by decreasing $^{87}\text{Sr}/^{86}\text{Sr}$ (0.70577 to 0.70373) and increasing $^{143}\text{Nd}/^{144}\text{Nd}$ (0.51234 to 0.51264) ratios over time in some segments. The close spatial relationship between arc magmatism, large-scale shear zones, and related strike-slip sedimentary basins in the Timok and Pangyurishte segments indicates mild transtension in these central segments of the restored arc. In contrast, the Eastern Srednogie segment underwent strong orthogonal intraarc extension. Segmental distribution of tectonic stress may account for the concentration of rich porphyry Cu deposits in the transtensional segments, where lower crustal magma storage and fractionation favored the evolution of volatile-rich magmas.

Keywords: Magmatic arc, subduction magmatism, Apuseni-Banat-Timok-Srednogorie, ABTS belt, Carpathian, Balkan, zircon, U-Pb geochronology, geochemistry

1. Introduction

Magmatic arcs form above active subduction zones at convergent plate boundaries, where a continental or oceanic plate margin overrides a subducting oceanic plate. Along a subduction zone, continental and oceanic arcs generally form distinct segments [e.g., *Mahlburg Kay et al.*, 1982; *Hildreth and Moorbath*, 1988]. In continental-margin arcs, the style of tectonic deformation may differ among segments along the arc and may also vary perpendicular to the arc in response to differences in preexisting geology, convergence rate and direction, or heterogeneities within the subducting plate. For example, along-arc differences among segments have been attributed to subducting ridges [*Cross and Pilger*, 1982; *von Huene and Ranero*, 2009], slab tear [*Wortel and Spakman*, 2000; *Rosenbaum et al.*, 2008], or flat-slab subduction of young oceanic lithosphere [*Haschke et al.*, 2002; *Kay and Coira*, 2009; *Ramos and Folguera*, 2009]. Across-arc variations in style and composition of magmatism may be related to steepening or shallowing of the subducting slab [e.g., *Trumbull et al.*, 2006], which can be related to changing rates or angles of plate convergence. The composition of subduction-related mantle magmas may vary as a result of heterogeneous source enrichment, and especially in continental arcs, will be modified by mineral fractionation and crustal assimilation processes, which occur primarily in the lower crust and on further ascent through the mature continental crust [*de Paolo*, 1981; *Hildreth and Moorbath*, 1988; *Annen et al.*, 2006]. Igneous geology and geochemistry can be used to identify magma sources and evolution processes and thus serve as evidence to interpret the large-scale plate-tectonic setting of complex arcs.

Subduction-related magmatic arcs are frequently endowed with magmatic-hydrothermal porphyry Cu ± Au ± Mo and epithermal Au ± Ag ± Cu deposits, which can themselves be taken as tectonic indicators [*Sawkins*, 1972; *Sillitoe*, 1972; *Groves and Bierlein*, 2007]. These deposits usually occur in discrete belts and do not extend along the entire length of magmatic arcs. Barren and mineralized segments are thought to be due to large-scale variations in tectonic stress of the lithosphere, and well-endowed segments empirically correlate with flat-slab subduction, subduction of oceanic ridges, or subduction reversals [*Solomon*, 1990; *Cooke et al.*, 2005; *Rohrlach and Loucks*, 2005; *Rosenbaum et al.*, 2005]. Major porphyry deposits develop preferentially in arc segments that were subjected to a compressional stress state during ore deposit formation [*Sillitoe*, 1997; *Camus*, 2002; *Richards*, 2003; *Rohrlach and Loucks*, 2005; *Sillitoe and Perelló*, 2005; *Sillitoe*, 2010]. Horizontal compression can trap magmas in a lower crustal magma chamber, where high-pressure magmatic differentiation and cyclic replenishment lead to enrichment in volatiles and metal content. Compression also influences the development of upper crustal magma chambers, thus preventing volcanic eruption and unfocused loss of volatiles but favoring focused fluid release through intensely veined porphyry stocks [*Rohrlach and Loucks*, 2005; *Richards*, 2011; *Loucks*, 2014]. High magmatic water contents favor the crystallization of hornblende and suppress plagioclase crystallization in the lower crust [e.g., *Burnham*, 1979; *Lang and Titley*, 1998; *Richards et al.*, 2001; *Richards*, 2003; *Rohrlach and Loucks*, 2005; *Chiaradia*, 2009]. Magmas which have evolved through these processes therefore have distinct geochemical signatures, generally referred to as “adakite-like”, which are characterized by high Sr/Y ratios, low Y concentrations, high light/heavy rare Earth element ratios (LREE/HREE), and weak or absent Eu anomalies [*Kay et al.*, 1999; *Richards et al.*, 2001; *Rohrlach and Loucks*, 2005; *Richards and Kerrich*, 2007; *Richards*, 2011].

The Eurasian continental margin includes one of the world's longest magmatic arc systems [Jankovic, 1997; Perelló *et al.*, 2008; Richards *et al.*, 2012; Richards, 2015], second only to the circum-Pacific region [Garwin *et al.*, 2005; Sillitoe and Perelló, 2005]. Unlike the circum-Pacific, which is dominated by long-lasting subduction of oceanic plates below continents, the magmatic arcs of Eurasia are embedded in the Alpine-Himalayan intra-continental orogenic system (Figure 1). Arc magmatism was driven by subduction of the Neotethys Ocean in Mesozoic to Tertiary times but terminated at the time of collision and was subsequently heavily overprinted by major collision-related deformations [Dewey *et al.*, 1973; Schmid *et al.*, 2008]. This collisional overprinting makes the reconstruction and interpretation of arc magmatism and the associated geotectonic setting more difficult [Sosson *et al.*, 2010; Bouilhol *et al.*, 2013]. The Late Cretaceous Apuseni-Banat-Timok-Srednogorie (ABTS) belt in southeastern Europe is the westernmost arc in the Alpine-Himalayan orogenic system related to the subduction of Neotethys [e.g., Berza *et al.*, 1998; Popov *et al.*, 2002]. This magmatic arc extends over 1000 km length from the Apuseni Mountains of Romania, through Serbia and Bulgaria to the Black Sea (Figure 1), finding a continuation not discussed in this contribution all the way to Iran. It was deformed after emplacement on a lithospheric scale [e.g., Neubauer, 2002]. Five segments that show distinct magmatic and mineralization trends can be distinguished along this arc (Figure 2). The timing and evolution of the magmatism and its associated ore deposits are well studied in the central and eastern segments [von Quadt *et al.*, 2005; Kamenov *et al.*, 2007; Peytcheva *et al.*, 2008; Georgiev *et al.*, 2009b; Kouzmanov *et al.*, 2009; Peytcheva *et al.*, 2009; Georgiev *et al.*, 2012; Kolb *et al.*, 2013]. However, information on the northwestern Banat and Apuseni segments is still scarce [Zimmerman *et al.*, 2008]. This hampers the establishment of a larger-scale model of the arc that also takes account of the regional tectonic and geophysical constraints.

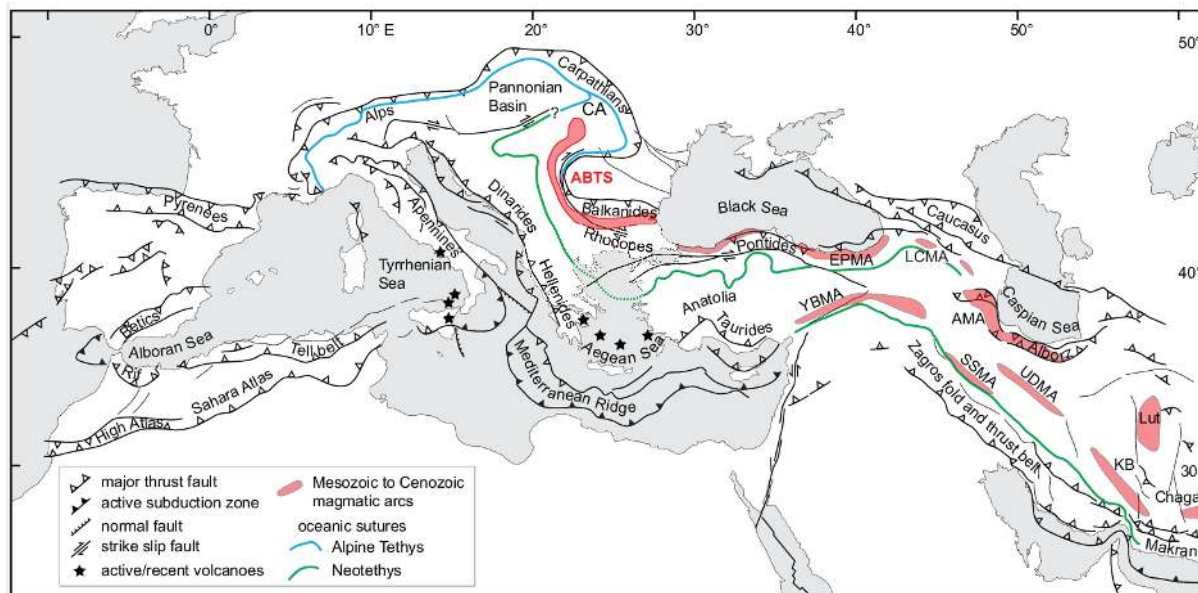


Figure 1. Tectonic sketch map of western Eurasia (modified from Morelli and Barrier [2004]). Major Late Tertiary to active thrust belts, active subduction zones, and recent arc volcanoes are shown in black; the sutures of the Neotethys (green) and location of Mesozoic to Oligocene arc magmas (red) are highlighted: ABTS Apuseni-Banat-Timok-Srednogorie belt, Alborz magmatic arc, Carpathian magmatic arcs, Eastern Pontide magmatic arc, Kerman belt, Lesser Caucasus magmatic arc, Sanandaj-Sirjan magmatic arc, Urumieh-Dokhtar magmatic arc, Yüsekova-Baskil magmatic arc.

Here we present new U-Pb ages, whole rock major and trace element analyses, and Sr and Nd isotopic data for the northern Banat and Apuseni segments and combine these new findings with those from previous studies. Comparing the geochemical characteristics along the arc reveals

similarities and differences between arc segments and identifies common magmatic processes that were active in all segments. We then use our extensive geochronological data set, to test and improve reconstructions of the Late Cretaceous paleotectonic evolution of the belt [e.g., *Neubauer, 2002; Fügenschuh and Schmid, 2005*]. Furthermore, we combine geochronological data with tectonic constraints derived from comagmatic sedimentary basins and fault systems to refine the large-scale tectonic history of the ABTS belt.

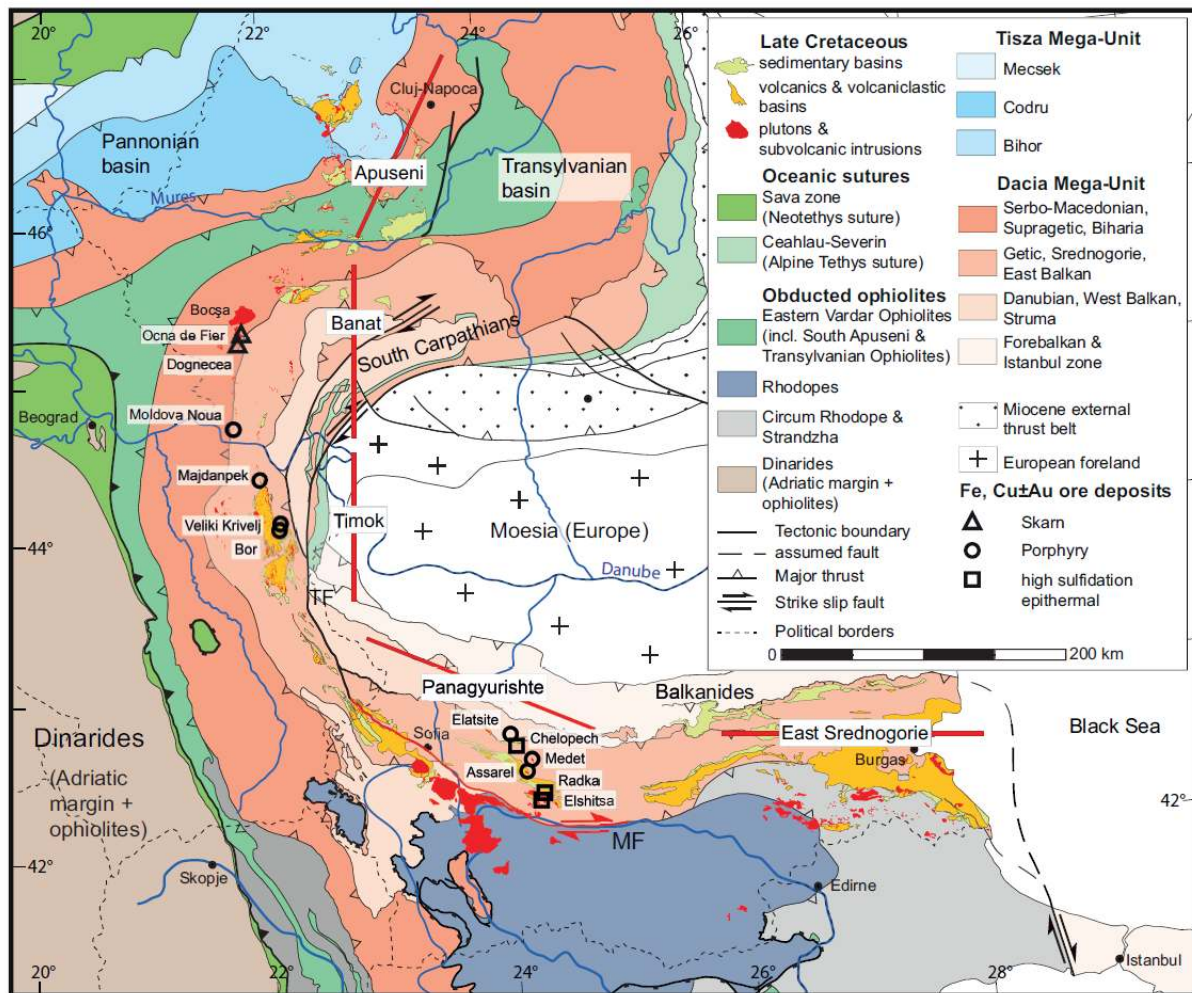


Figure 2. Geological map of the Carpathian-Balkan orogen, modified from *Schmid et al. [2008; 2011]*, showing major tectonic units and the occurrences of Late Cretaceous igneous rocks and sedimentary basins grouped into five segments of ABTS belt. These are, from NW to SE, the Apuseni, Banat, Timok, Panagyurishte, and Eastern Srednogorie segments. The red bars are the reference lines approximating the present-day orientation of the arc front in each of the five segments, based on geochronological data derived in this and previous studies. MF = Maritsa fault system and TF = Timok fault are major transverse structures used to separate the segments.

2. Regional Geology

The Late Cretaceous magmatic arc and associated metallogenic belt crop out in the Balkan, Northern Rhodopes, South Carpathian, and Apuseni mountain ranges, which generally rise to less than 2000 m above sea level and are partly obscured by Miocene to recent sediments of the Pannonian Basin. The subduction-related igneous rocks intruded previously assembled tectonic units, and they discordantly cross older nappe boundaries (Figure 2) (modified from *Schmid et al. [2008]*). The arc was intensely deformed after its emplacement and bent around the Moesian platform to create the present L shape of the arc [e.g., *Ratschbacher et al., 1993; Fügenschuh and Schmid, 2005; Ustaszewski et al., 2008; van Hinsbergen et al., 2008*], but this deformation was not pervasive and was confined to brittle fault structures and ductile shear zones at the current level

of exposure. The complex interplay of compressional and extensional tectonics which partly predated, and partly overprinted the Late Cretaceous magmatic arc, gave rise to the distinct segments of ABTS belt: Apuseni, Banat, Timok, Panagyurishte, and Eastern Srednogorie segments, which we define here based on geographic region and major crustal fault zones (Figure 2).

2.1. Tectonic Units of the Carpathian-Balkan Orogen

The Carpathian-Balkan orogen formed due to subduction of oceans and collision of continental blocks with the European continental margin, which was driven by the overall convergence between the African and European plates [e.g., *Boccaletti et al.*, 1974; *Herz and Savu*, 1974; *Csontos and Vörös*, 2004; *Schmid et al.*, 2008; *Matenco et al.*, 2010; *Schmid et al.*, 2011]. The Moesian platform represents the undeformed European foreland and was amalgamated with other units derived from the European margin (Tisza and Dacia Mega-Units) in mid-Cretaceous times [*Săndulescu*, 1984; 1994; *Schmid et al.*, 2008]. The nonophiolitic parts of the Dinarides became detached from the Adriatic microplate that separated from the African plate during the Mesozoic within the present-day South Mediterranean realm [*Handy et al.*, 2010; *Marton et al.*, 2010]. All the continental units that host the ABTS belt are located north and east of the Europe-Adria suture (Sava zone; see Figure 2) and were originally derived from the European plate. This relationship holds for the Dacia Mega-Unit encompassing the major units of the South Carpathians which continue into the Balkan orogen in Bulgaria [*Csontos and Vörös*, 2004; *Schmid et al.*, 2008] and for the continental Tisza Mega-Unit, poorly exposed in isolated inselbergs within the Pannonian Basin and in the Apuseni Mountains of Romania [*Csontos and Vörös*, 2004; *Haas and Pero*, 2004; *Kounov and Schmid*, 2013]. Although the origin of the Strandzha, Circum-Rhodope, and the Rhodope Units is somewhat ambiguous, they certainly have been part of the European continental margin since at least Cretaceous times [*Okay et al.*, 2001; *Schmid et al.*, 2008; *Burg*, 2011]. The Rhodope Unit is separated from the Dacia Mega-Unit along the right-lateral Maritsa fault system that comprises several NW-SE trending shear zones, among others the Iskar-Yavoritsa shear zone, which became active in the Late Cretaceous [*Georgiev et al.*, 2009a; *Naydenov et al.*, 2013].

Two domains of oceanic lithosphere, Neotethys and Alpine Tethys, opened in Triassic and Jurassic times, respectively. Their remnants denote distinct paleogeographic realms (Figure 1). Opening of the Alpine Tethys was kinematically linked to the opening of the central Atlantic. The main branch of Alpine Tethys forms an oceanic suture in the Alps and Western Carpathians that links with the Neotethys suture of the Sava zone across the mid-Hungarian shear zone. A second branch led to the suturing of the Ceahlau-Severin Ocean of the East and South Carpathians that can only be followed until the Serbian-Bulgarian border (Figures 1 and 2) [*Kräutner and Krstić*, 2002; *Schmid et al.*, 2008; *Matenco et al.*, 2010]. The Alpine Tethys was too narrow to give rise to subduction-related arc magmatism during its closure, and it was proposed that intrusions in the Alps were related to slab break-off [cf. *Davies and von Blanckenburg*, 1995]. Miocene and younger calc-alkaline magmas in the Carpathians are related to postcollisional extension or lithospheric delamination [*de Boorder et al.*, 1998; *Seghedi et al.*, 1998; *Harangi and Lenkey*, 2007; *Fillerup et al.*, 2010; *Seghedi and Downes*, 2011]. The Neotethys suture is located between units of the European continental margin (Tisza and Dacia Mega-Units) and the Adriatic margin (Dinarides) [*Schmid et al.*, 2008]. Before final collision between Europe and Adria, two different parts of the Neotethys were obducted during the latest Jurassic. The Eastern Vardar ophiolitic sheets were obducted onto the Tisza and Dacia Mega-Units, while the Western Vardar sheet was emplaced onto the Adria-derived Dinarides [*Csontos and Vörös*, 2004; *Schmid et al.*, 2008; *Kounov and Schmid*, 2013]. Final closure of the main branch of Neotethys along the Sava Neotethys suture occurred at the end of the Cretaceous [*Pamić*, 2002; *Karamata*, 2006; *Ustaszewski et al.*, 2010],

after a long period of north dipping subduction of the remnants of the Neotethys Ocean, attached to the Adria margin in the south, underneath the Europe-derived Tisza and Dacia Mega-Units. According to most authors, it is this originally north dipping subduction of Neotethys that gave rise to the magmatism in the ABTS belt analyzed in this study. After collision at the end of the Cretaceous, intracontinental convergence continued in Cenozoic times, which led to the severe oroclinal bending of the ABTS belt, as seen in Figure 2 [Fügenschuh and Schmid, 2005].

2.2. Prearc Nappe Assemblage and Postarc Tectonic Modifications

Because the Late Cretaceous ABTS belt cuts across the boundaries between different tectonic units (Figure 2), it is obvious that this magmatic arc of the Carpathian-Balkan orogen was preceded by several earlier and distinct compressional phases. These compressional phases partly involved closure of small oceans leading to collision and nappe stacking within the European continental margin but not to arc magmatism. The north facing Strandzha and Circum-Rhodope Units were intensely deformed and regionally metamorphosed during a latest Jurassic to earliest Cretaceous orogeny [Okay et al., 2001; Bonev and Stampfli, 2011]. At about the same time, parts of the nappe stack of the Rhodope unit formed [Ricou et al., 1998; Bonev et al., 2006; Burg, 2011], associated with a first event of eclogitization within what is referred to as the Rhodope Suture Zone or Nestos suture [Krenn et al., 2010; Turpaud and Reischmann, 2010]. A second compressional phase in the Early Cretaceous (~130–100 Ma, “Austrian” phase) led to subduction of the narrow Ceahlau-Severin Ocean (Alpine Tethys; Figure 2), to collision associated with, in present-day coordinates, northeast facing nappe stacking within the Dacia Mega-Unit [e.g., Schmid et al., 1998; Iancu et al., 2005] and south directed synmetamorphic thrusting in the Rhodopes [Burg, 2011]. This event is recorded by $^{40}\text{Ar}/^{39}\text{Ar}$ cooling ages in the Getic-Supragetic, Srednogorie, and Biharia Units [Dallmeyer et al., 1996; Dallmeyer et al., 1999; Velichkova et al., 2004; Kounov et al., 2010]. A subsequent Cretaceous tectonic phase affected the Tisza Mega-Unit in the Turonian (~94 to 90 Ma) forming the present-day nappe stack of the Apuseni Mountains, followed by extension that formed Gosau-type postorogenic basins (Figure 2) from the Late Turonian onward [Schmid et al., 2008; Kounov and Schmid, 2013], synchronous with the magmatic activity in the ABTS belt. Thrusting during the latest Cretaceous was associated with the thrusting of the internal units of the Dacia nappe stack eastward over the Danubian nappes and with only minor deformation in the Apuseni Mountains and most parts of the Dacia Mega-Unit (Late Campanian-Maastrichtian) [Săndulescu, 1984; Iancu et al., 2005; Schmid et al., 2008; Kounov and Schmid, 2013], which only mildly affected the ABTS belt. However, most of the oroclinal bending of the Dacia and Tisza Mega-Units, together with the originally straight ABTS belt they host, occurred in Cenozoic times [Fügenschuh and Schmid, 2005; Ustaszewski et al., 2008] and in the framework of the invasion of the Tisza and Dacia Mega-Units into the Carpathian embayment [Balla, 1987; Csontos and Vörös, 2004].

2.3. The Late Cretaceous Magmatic Arc

Calc-alkaline magmatism was initiated after the Austrian phase when the Lower Cretaceous Europe-verging nappe stack preserved within Tisza and Dacia became an upper plate continental unit above the north dipping subduction zone of the Neotethys lower plate. The magmatic arc can be divided into five segments (Figure 2), based on structurally observed boundaries and published geological mapping.

The northernmost, presently NNE-SSW trending (1) Apuseni segment extends from volcanics outcropping within the Tisza Mega-Unit to small plutons emplaced in the Eastern Vardar ophiolitic unit. The (2) Banat segment is located south of the Apuseni segments and the Eastern

Vardar ophiolitic unit. The mostly plutonic rocks of the Banat segment crop out exclusively within the Dacia Mega-Unit of the Banat area in Romania. The Danube is the natural boundary between the Banat segment and the (3) Timok segment. The adjacent (3) Timok segment differs from the Banat segment in being preserved at a higher erosion level, as indicated by abundant volcanic rocks and volcanoclastic basins, richly mineralized porphyries, and the abundant occurrence of adakite-like rocks [Ciobanu *et al.*, 2002; Kolb *et al.*, 2013]. The Timok and (4) Panagyurishte segments are divided from each other by the Cenozoic right-lateral Timok Fault that links with the Late Cretaceous right-lateral Maritsa fault system (Figure 2). All igneous products to the east of the Timok Fault are attributed to the Panagyurishte segment. The Panagyurishte segment comprises West Bulgarian occurrences and stretches from the Elatsite deposit in the north to the Rila granitic pluton in the Rhodopes in the south [von Quadt and Peytcheva, 2005; Peytcheva *et al.*, 2007]. The separation of the Panagyurishte segment from the (5) Eastern Srednogorie segment is defined by a gap in magmatic activity that coincides with a reduction of crustal thickness toward the Eastern Srednogorie segment [Yosifov and Pchelarov, 1977], probably induced during rifting of the Black Sea [Görür, 1988] and persisting today. (5) The Eastern Srednogorie segment is the only segment that hosts potassium-rich primitive magmas [e.g., Georgiev *et al.*, 2009b] extruded in a marine intraarc rift basin. The Eastern Srednogorie segment is terminated by the Western Black Sea Fault, which shifted the Istanbul zone, formerly connected to the Prebalkan, to the south during the opening of the Black Sea [Okay *et al.*, 1994]. The magmatic arc continues into the Pontides, Lesser Caucasus, and into northern Iran outside the area of this study [e.g., Jankovic, 1997; Rice *et al.*, 2009; Sosson *et al.*, 2010].

The central Timok and Panagyurishte segments host economically significant porphyry-type and epithermal Cu-Au deposits [Ciobanu *et al.*, 2002; Heinrich and Neubauer, 2002], whereas skarn-type (calc-silicate replacement) and polymetallic vein deposits prevail in the three adjacent segments, the Apuseni, Banat and Eastern Srednogorie segments [Vlad, 1997; Berza *et al.*, 1998; Popov *et al.*, 2002]. Broadly coeval volcano-sedimentary basins and sedimentary basins (Gosau-type basins in Romanian literature) occur in all segments along the magmatic arc [Georgiev *et al.*, 2001; Willingshofer *et al.*, 2001; Popov *et al.*, 2002; Krättnner and Krstić, 2003; Schuller *et al.*, 2009].

3. Results

3.1. Sample Selection and Compilation of Data

We collected some 100 samples of Late Cretaceous igneous rocks from the northernmost Banat and Apuseni segments. The Late Cretaceous plutons, subvolcanic stocks, dikes, and volcanics are generally undeformed. The majority of samples are fresh and lack alteration, and weathered surfaces were removed prior to sample processing. Loss on ignition (LOI) values for the Banat and Apuseni samples range from 0.45 to 6.57 wt %, and 15 out of the 87 analyzed samples have a LOI higher than 3 wt %, which indicates moderate alteration. Higher LOI values might affect mobile elements (e.g., Sr, Pb, K, and Ba) but the variations of these elements are probably primary magmatic, because they do not correlate systematically with LOI. Whole rock samples were analyzed for major and trace elements and for Sr and Nd isotope ratios (see Text S1 in the supporting information for details). Additionally, we compiled geochemical whole rock data from previous studies of the Timok segment [Kolb *et al.*, 2013], the Panagyurishte segment [Kamenov *et al.*, 2003; Stoykov *et al.*, 2004; Chambefort *et al.*, 2007; Kamenov *et al.*, 2007; Peytcheva *et al.*, 2008; Kouzmanov *et al.*, 2009; Peytcheva *et al.*, 2009] and the Eastern Srednogorie segment [Georgiev *et al.*, 2009b]. Major and trace element data are reported in Table S1, and Sr and Nd isotopic data are reported in Table S2.

Samples showing clear temporal relations in the field, deduced from crosscutting relations or wall-rock contacts, were preferentially chosen for U-Pb age dating (see Text S1 for details). Single zircon crystals of 54 Late Cretaceous igneous rocks from the Banat and Apuseni segments were dated by the laser ablation–inductively coupled plasma–mass spectrometry (LA-ICP-MS) and/or thermal ionization mass spectrometry (TIMS) method. For both methods, crystallization ages were calculated from the dates of single zircon crystals and given as $^{206}\text{Pb}/^{238}\text{U}$ ages. Our new data are complemented by U-Pb ages for the Timok segment [Kolb, 2011; Kolb et al., 2013], the Panagyurishte segment [von Quadt et al., 2002; Kamenov et al., 2003; Stoykov et al., 2004; von Quadt et al., 2005; von Quadt and Peytcheva, 2005; Chambefort et al., 2007; Peytcheva et al., 2007; Peytcheva et al., 2008; Kouzmanov et al., 2009; Peytcheva et al., 2009; Atanasova-Vladimirova et al., 2010; Nedkova et al., 2012; Bidzhova et al., 2013] and the Eastern Srednogie segment [Georgiev et al., 2012]. Calculated crystallization ages for all segments are reported in Table S3. A tectonic map of the ABTS belt summarizing the crystallization ages of the magmatic samples is provided in Appendix Figure A1. LA-ICP-MS single zircon dates for the Banat and Apuseni segments are reported in Table S4, TIMS data are given in Table S5. Concordia and $^{206}\text{Pb}/^{238}\text{U}$ age weighted average plots are given in Figure S1 in the supporting information. We report 2 standard deviations (2σ) of overlapping and concordant TIMS or LA-ICP-MS ages in a population of analyses of each sample, as a conservative measure of age uncertainty, rather than standard errors of the mean that become unrealistically small in the case of numerous point analyses [von Quadt et al., 2011].

3.2. Geochemical Results

3.2.1. Major Elements and Classification

We classify volcanic, shallow intrusive (porphyritic to hypabyssal) and plutonic rocks from the ABTS belt according to their whole rock geochemistry. In the $A = \text{Na}_2\text{O} + \text{K}_2\text{O}$, $F = \text{FeO}$, $M = \text{MgO}$ (AFM) plot (Figure 3a) [Kuno, 1968; Irvine and Baragar, 1971] nearly all Late Cretaceous samples from the ABTS belt fall into the field of calc-alkaline rocks, with the exception of primitive magmas from the Eastern Srednogie segment, which fall into the tholeiite field on account of their exceptionally high Fe + Mg. For easier comparison, all volcanic and intrusive samples were plotted in the same total alkalis versus silica (TAS) diagram, subdivided and labelled for volcanic rock names only (Figure 3b) [Le Maitre et al., 1989]. Additional information about the igneous rock series can be inferred from the K_2O versus SiO_2 diagram (Figure 3c) [Rickwood, 1989]. The samples show a wide compositional range from basalt to rhyolite with a predominance of andesite to dacite magmas. The majority of Apuseni samples have SiO_2 contents over 60 wt %, fall into the dacite and rhyolite fields, and belong to the high-K calc-alkaline series. The Banat samples are mostly intermediate to acid rocks and plot in the calc-alkaline and high-K calc-alkaline fields. Timok segment samples are predominantly intermediate in silica but comprise calc-alkaline to shoshonite series [Kolb et al., 2013]. The Panagyurishte samples show a wide compositional variation and fall into the fields of calc-alkaline and high-K calc-alkaline series. Basic to intermediate magmas predominate in the Eastern Srednogie segment. Samples from the central part of this segment are particularly enriched in alkalis ($\text{Na}_2\text{O} + \text{K}_2\text{O}$) and hence belong to the high-K calc-alkaline and shoshonite series [Georgiev et al., 2009b].

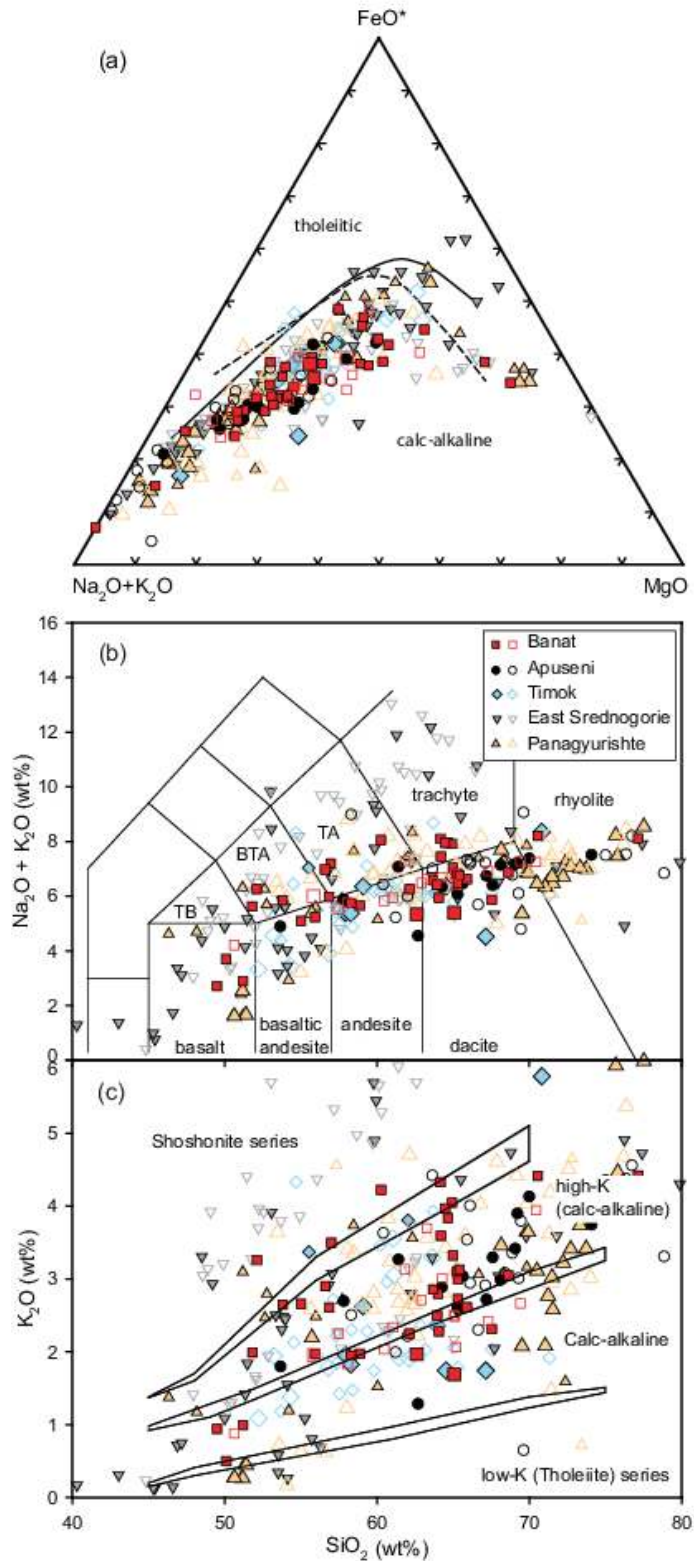


Figure 3. Chemical classification of Late Cretaceous igneous rocks from different segments of the ABTS belt (see inset of Figure 3b). The open symbols denote the volcanic and shallow intrusive rocks, and the filled symbols indicate the plutonic rocks. The larger symbols indicate the samples related to ore deposits. **(a)** AFM diagram showing the boundary between calc-alkaline and tholeiitic series after *Kuno* [1968] (solid line) and *Irvine and Baragar* [1971] (stippled line). **(b)** Total alkalis versus silica (TAS) diagram [*Le Maitre et al.*, 1989]. TB: trachybasalt, BTA: basaltic trachyandesite, TA: trachyandesite. **(c)** K₂O versus SiO₂ classification diagram for subalkalic rocks, boundary bands after *Rickwood* [1989]. Analyses in Figures 3b and 3c were recalculated to 100% on an H₂O-free basis.

3.2.2. Trace Element Characteristics

The individual arc segments have different concentrations of trace elements which may be explained by mineral fractionation (see section 4.1 for discussion) (Figure 4). Light rare Earth elements (LREE, e.g., La and Ce) are moderately enriched in the ABTS belt samples and pronounced Eu anomalies are largely absent ($\text{Eu}/\text{Eu}^* 0.8\text{--}1.2$) for the majority of samples with less than 65 wt % SiO_2 (Figure 4a). In normal mid-ocean ridge basalt (N-MORB)-normalized [Sun and McDonough, 1989] trace element plots (Figure 4b), samples from all five segments show enrichment in large-ion lithophile elements (LILEs), such as Ba, K, Sr, and Pb; somewhat less enrichment in U and Th; and depletion of Nb, Ta, and other high field strength elements (HFSEs, e.g., Zr and Hf).

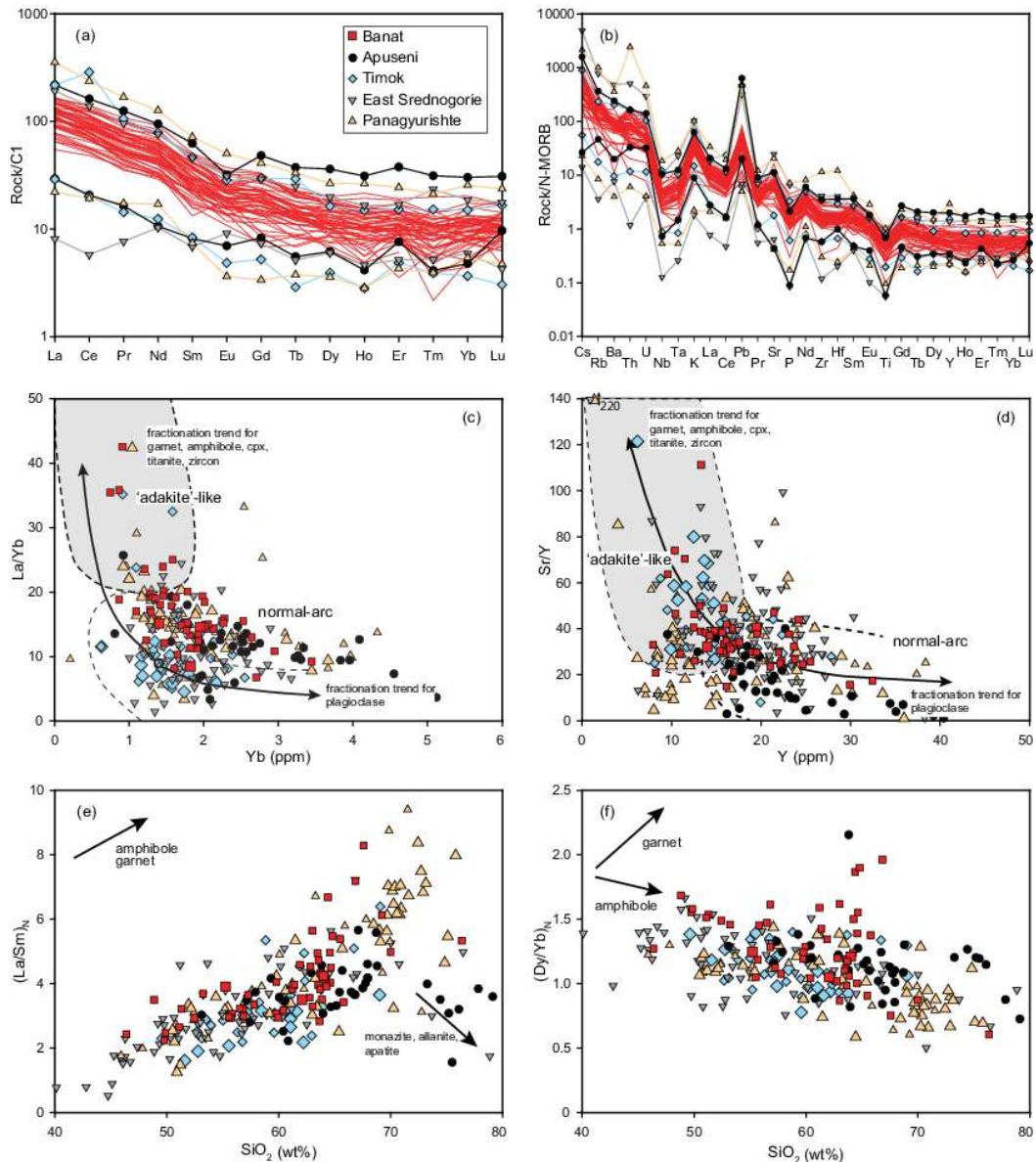


Figure 4. Trace element characteristics of Late Cretaceous igneous rocks from ABTS belt. **(a)** Chondrite-normalized rare Earth elements. All samples from Banat segment are plotted (red lines); for the other arc segments the overall range of data is represented by lines for the maximum and minimum values. **(b)** N-MORB-normalized trace element patterns. Normalizing values for Figures 4a and 4b from Sun and McDonough [1989]. Trace element ratios: **(c)** La/Yb versus Yb. **(d)** Sr/Y versus Y (ppm) and the fields for adakite-like and normal-arc magma compositions (from Defant and Drummond [1993]) and qualitative differentiation paths of various minerals (from Richards and Kerrich [2007]). **(e)** $(\text{La}/\text{Sm})_N$ and **(f)** $(\text{Dy}/\text{Yb})_N$ versus SiO_2 (wt%) as a measure of fractionation, with mineral fractionation paths from Davidson et al. [2007].

The plots of La/Yb versus Yb and Sr/Y versus Y (Figures 4c and 4d) aim at distinguishing normal-arc magmas from adakite-like signatures defined by La/Yb and Sr/Y ratios in excess of 20 and Yb and Y contents below 1.9 and 18 ppm, respectively [Defant and Drummond, 1993; Richards and Kerrich, 2007]. Apart from some Timok, Banat, and Panagyurishte samples, most samples plot in the normal-arc field in the La/Yb plot (Figure 4c). The Sr/Y plot, however, shows more variation among the arc segments. The majority of samples from Panagyurishte and Banat segments fall into both fields, close to the field limits; some Panagyurishte samples with low Y contents fall below the adakite-like Sr/Y. Eastern Srednogorie and Timok samples partly fall into the normal-arc field but also display adakite-like affinities with higher Sr/Y ratios. Apuseni samples mainly plot in the normal-arc field. Rare Earth element ratios, $(La/Sm)_N$ and $(Dy/Yb)_N$, plotted versus SiO_2 can give insights into mineral fractionation (Figures 4e and 4f). The $(La/Sm)_N$ ratios of ABTS belt samples generally increase with increasing SiO_2 ; the Apuseni samples show a decrease at SiO_2 contents higher than 70 wt %. $(Dy/Yb)_N$ ratios decrease with increasing SiO_2 in all arc segments.

3.2.3. Isotope Geochemistry

Age-corrected Sr_i isotope ratios and ϵNd_i values show a significant variation among the arc segments. Nevertheless, individual segments partly overlap. The data lie between the mid-ocean ridge basalt (MORB)-type mantle source field (Timok) and that of Variscan granitoids (Apuseni) from the prearc European basement [Duchesne et al., 2008]. The Timok samples are the least radiogenic (highest ϵNd_i : +4.4 to +5.4 and lowest $^{87}Sr/^{86}Sr_i$: 0.70339 to 0.70375) [Kolb et al., 2013]; the more radiogenic Timok samples overlap with the isotopically primitive Banat samples. Banat samples extend to highly radiogenic isotopic compositions (low ϵNd_i : -1.8 to -3.1 and high $^{87}Sr/^{86}Sr_i$: 0.70598 to 0.70707) and partly overlap with the basement granitoids. Panagyurishte samples are also part of this array and overlap with or are slightly more radiogenic than the Banat samples. However, a few Panagyurishte samples are shifted off this trend toward more primitive Sr_i isotope ratios at low ϵNd_i values (-1.7 and lower). Age-corrected Sr_i isotope ratios (not plotted in Figure 5) for the Eastern Srednogorie segment range from 0.70392 to 0.70590 and overlap with the other segments.

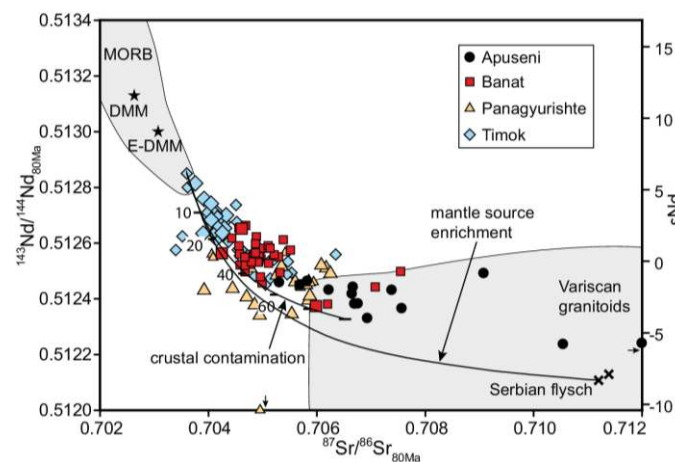


Figure 5. Initial Sr and Nd isotope ratios for samples from the Late Cretaceous ABTS belt. Samples from Banat, Timok, and Eastern Srednogorie segments were backcalculated to 80 Ma based on analyzed bulk Rb and Sm concentrations; Panagyurishte samples were corrected for 85 Ma and 90 Ma (Table S2). (a) ϵNd_i versus $^{87}Sr/^{86}Sr_i$. Field for MORB from Stracke et al. [2005], composition of depleted MORB mantle (DMM) and enriched DMM from Workman and Hart [2005], field for Variscan granitoids (corrected to 80 Ma) from Duchesne et al. [2008] and Peytcheva et al. [2008], and composition of Serbian flysch sediments from Prelevic et al. [2008]. Two-component isotopic mixing for mantle source enrichment between isotopically unmodified, least radiogenic Timok sample (MM38) [Kolb et al., 2013] and Serbian flysch (06FL03) [Prelevic et al., 2008]. Mixing line for crustal contamination shows percent addition of representative basement gneiss (R4626) [Duchesne et al., 2008] to the presumably isotopically unmodified, least radiogenic Timok sample (MM38) [Kolb et al., 2013]; see text for discussion.

3.3. Age Constraints

3.3.1. Timing of Magmatic Activity

All arc segments were simultaneously active over the time period of 81 to 75 Ma (Campanian), but onset and termination of magmatic activity occurred at different times in the individual segments (Figure 6 and Table S3). Magmatic activity along the ABTS belt started as early as ~92 Ma (Turonian) in the northern Panagyurishte segment [von Quadt *et al.*, 2002; Stoykov *et al.*, 2004; Chambefort *et al.*, 2007; Kamenov *et al.*, 2007]; it set in slightly later, between 90 and 87 Ma, in the Timok and Eastern Srednogorie segments [Kolb, 2011; Georgiev *et al.*, 2012]. In the Banat and Apuseni segments, magmatism apparently did not start before ~84 and ~81 Ma, respectively. The youngest igneous products occur in the Banat and Timok segments (74 to 71 Ma). However, still younger magmatism is found in the Rhodope Unit, which forms the southern parts of the Panagyurishte and Eastern Srednogorie segments (67-71 Ma) [von Quadt and Peytcheva, 2005; Marchev *et al.*, 2006; Peytcheva *et al.*, 2007]. Our compilation includes only the Late Cretaceous magmatism in the Rhodope Unit, although magmatism continued beyond the Cretaceous-Palaeogene boundary, used as a somewhat arbitrary limit of our compilation in this area.

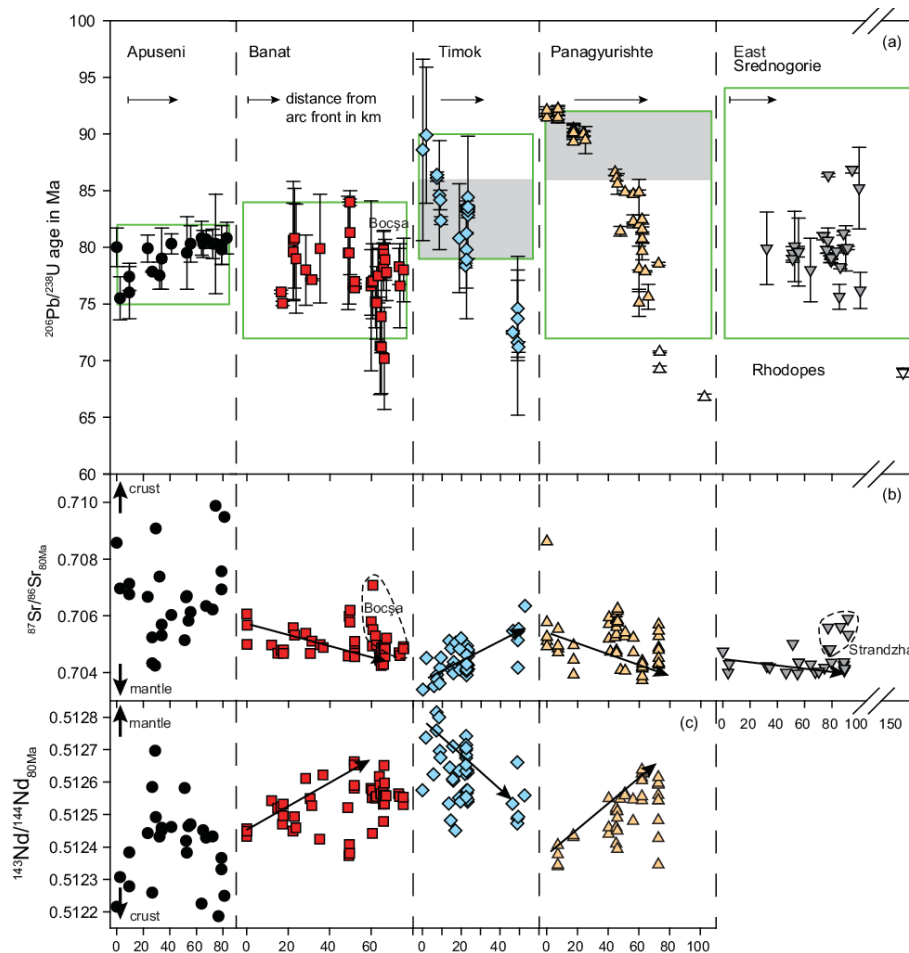


Figure 6. (a) Compilation of $^{206}\text{Pb}/^{238}\text{U}$ ages (in Ma) for ABTS belt and Rhodopes (see Table S3 for sources). The five segments of ABTS belt are arranged along the arc from northwest (Apuseni) to southeast (Eastern Srednogorie). Within the individual segments, data points are sorted in terms of increasing distance in km from the inferred arc front (red reference lines in Figure 2), which corresponds to a sorting from paleo-north to paleo-south after restoration of the L-shaped bend in the magmatic arc (see text for explanation). The grey bands indicate the more restricted intervals of magmatic-hydrothermal Cu \pm Au mineralization in the Timok and Panagyurishte segments. The green frames indicate the sedimentation intervals in comagmatic basins. **(b)** Corresponding across-arc trends of $^{87}\text{Sr}/^{86}\text{Sr}_i$ ratios. This compilation also includes $^{87}\text{Sr}/^{86}\text{Sr}_i$ ratios of samples for which no U-Pb ages are available. Two Apuseni samples (DG094 and DG112) fall outside the plotted Sr isotope ratio range, further emphasizing the unusually wide range in this segment. **(c)** Corresponding across-arc trends of $^{143}\text{Nd}/^{144}\text{Nd}_i$ ratios.

3.3.2. *Across-Arc Age Progression and Isotope Variation*

Some arc segments show distinct across-arc age variations, whereby geochemical distribution patterns vary in correlation with the age of magma emplacement. However, because trace elements might be affected by differentiation, we focus on isotopic variations only. We use the red reference lines approximating the orientation of the arc front in each segment (Figure 2) to sort the ages and isotopic compositions within the arc segments. We start with samples close to these lines and move perpendicular to the reference line toward northwest in the Apuseni segment, to the west in the Banat and Timok segments, to the southwest in the Panagyurishte segment, and to the south in the Eastern Srednogorie segment (Figure 6, from left to right).

The Timok and Panguurishte segments show the most pronounced progression of magmatic activity (Figure 6), which is also clearly visible in the age-distribution map included in Appendix 1 of this paper. The oldest ages occur closest to the interpreted arc magmatic front; in each segment, the youngest magmatic ages are found furthest away from the arc front [von Quadt *et al.*, 2005; Kolb *et al.*, 2013]. In the Eastern Srednogorie segment, ages show no clear overall trend, but the oldest intrusions tend to occur in the southern periphery (Strandzha Unit) of the region exposing overall younger, submarine extrusive rocks [Georgiev *et al.*, 2012]. Magmatism in the Rhodope Unit (67–71 Ma) [von Quadt and Peytcheva, 2005; Marchev *et al.*, 2006; Peytcheva *et al.*, 2007] is interpreted as the continuation of the magmatic activity in the Panagyurishte and Eastern Srednogorie segments. Within the Banat segment younging of magmatism toward the west from 83.9 to 70.2 Ma is only observed in the area that is currently adjacent to Serbia. By contrast, two samples from the northern part located close to the inferred arc front yield younger ages (75–76 Ma), and the large Bocşa pluton and close-by smaller intrusions that occur furthest away from the inferred arc front yield distinctly older ages (76 to 80 Ma). In the Apuseni segment, where the youngest ages (75.5 to 78 Ma) are found closest to the inferred arc front, the trend in age progression appears to be reversed.

The across-arc age trends are accompanied by distinct geochemical changes, which are most clearly traced by isotopic signatures. The Panagyurishte magmatism evolves toward lower $^{87}\text{Sr}/^{86}\text{Sr}_i$ ratios and higher ϵNd_i south-wards, and the most depleted isotopic compositions are found in the youngest samples [von Quadt *et al.*, 2005]. A similar evolution to more primitive Sr and Nd isotopic ratios away from the arc front is found in the Banat segment. Magmatism in the Timok segment, however, evolves towards more radiogenic Sr and less radiogenic Nd isotope ratios away from the arc front, as well as in time, but is briefly interrupted by a shift to lower $^{87}\text{Sr}/^{86}\text{Sr}_i$ ratios and higher ϵNd_i at ~83 Ma [Kolb *et al.*, 2013]. The $^{87}\text{Sr}/^{86}\text{Sr}_i$ ratios in the Eastern Srednogorie segment are relatively low and vary little in the central rifted basin, whereas higher ratios are found in the southern part (Strandzha Unit), which includes older intrusives in this segment [Georgiev *et al.*, 2009b]. No clear isotopic trend is observed in the Apuseni samples. Some volcanic rocks have particularly high $^{87}\text{Sr}/^{86}\text{Sr}_i$ ratios, whereas the youngest rocks coincide with relatively low $^{87}\text{Sr}/^{86}\text{Sr}_i$ ratios.

4. Discussion

This discussion aims at supporting and refining the idea that the geochemical characteristics of the different arc segments are best explained by a single north dipping subduction zone of the Neotethys Ocean (also referred to as the “Vardar” Ocean) that was active during the Late Cretaceous and was closed by collision of the Adriatic microcontinent with the European plate [e.g., von Quadt *et al.*, 2005; Georgiev *et al.*, 2012; Kolb *et al.*, 2013]. Subduction induced magmatism within this northerly adjacent continental upper plate but also created distinct magmatic and

metallogenetic characteristics for each segment of the magmatic arc. First, we will discuss the tectonic significance of our compilation of geochemical and geochronological data. Next, we will refine the tectonic reconstruction of this arc (Figure 7), prior to its large-scale bending into the present-day L shape by deformations occurring during and after continental collision.

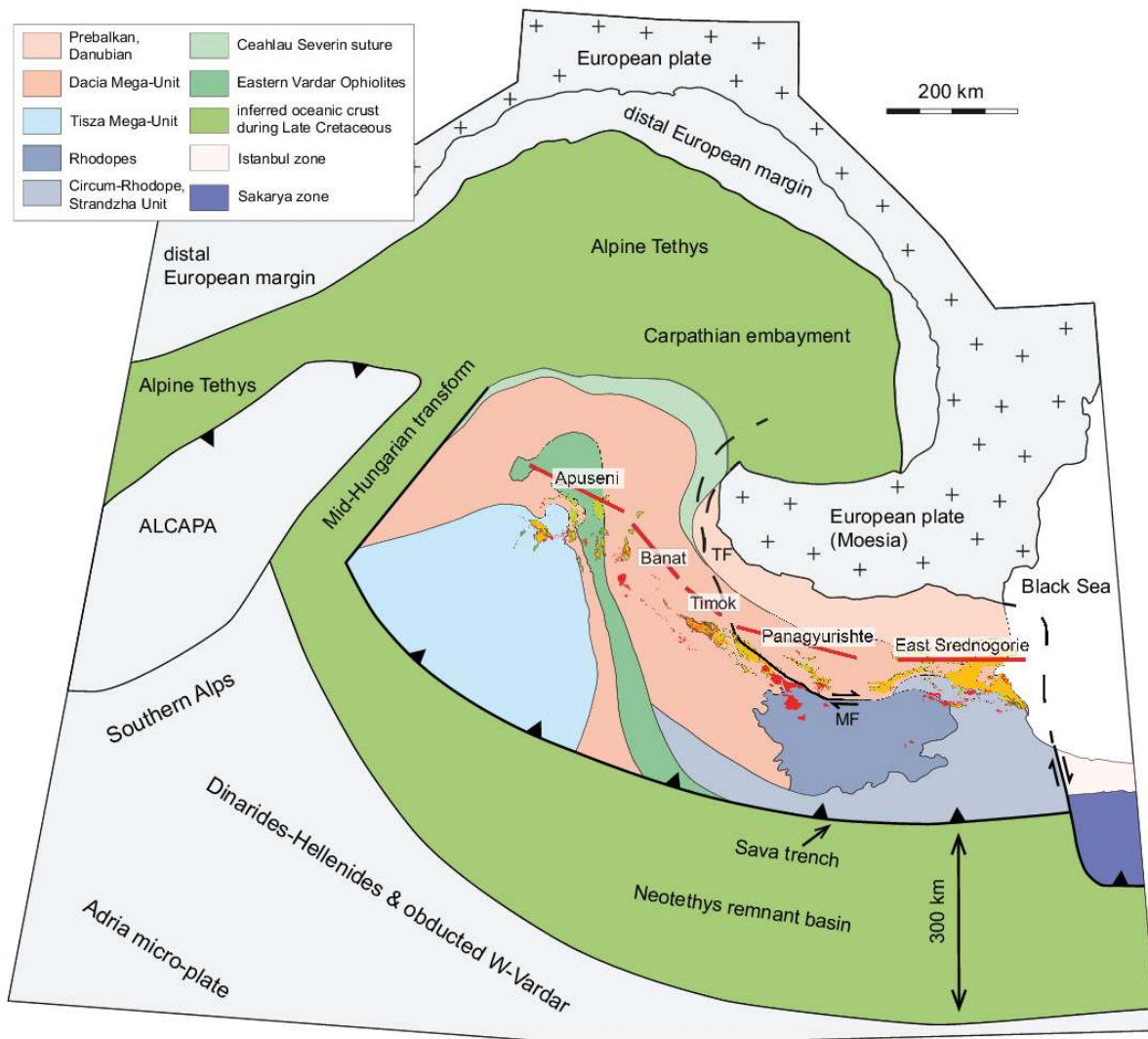


Figure 7. Restoration of the configuration at the onset of arc magmatism around 90 Ma ago, partly based on retrodeformations of *Ustaszewski et al.* [2008] and *Fügenschuh and Schmid* [2005] but modified to restore the magmatic arc to a gently curved line, consistent with paleomagnetic data. TF = Timok fault, MF = Maritsa fault system. The straight red lines are the reference lines for the individual arc segments, with the same orientation relative to outcropping magmatic bodies as shown in Figure 2.

4.1. Tectonic Significance of Magma Geochemistry and Magmatic Ages

Subduction-related mantle melts that ascend through mature continental crust undergo fractionation and crustal contamination, which modifies their original composition [*de Paolo*, 1981; *Hildreth and Moorbath*, 1988; *Thirlwall et al.*, 1996]. Therefore, tracing the primary source(s) of magmas in an evolved arc is difficult. Magmatism in all segments of the ABTS belt shows a clear “arc signature”, i.e., enrichment in LILE (Ba, K, Sr, and Pb) and depletion in HFSE (Nb, Ta, Zr, and Hf; Figure 4a and 4b), which is also prominent in the less evolved basaltic andesites and indicates a subduction-related origin of the magmas.

The observed isotopic compositions in the ABTS arc magmas indicate interaction with continental crust (Figure 5). Theoretically, some crustal contamination might have already taken place in the

mantle source via addition of subducted sediment [Elliott, 2003]. In a continental arc, however, evolved isotopic compositions are more likely acquired during interaction and assimilation of the local continental crust [Hildreth and Moorbath, 1988; Wörner et al., 1992]. The local continental crust [Duchesne et al., 2008] and subducted sediments [Prelevic et al., 2008] are isotopical rather similar in this region, which impede any further distinction, but most of the contamination might have occurred during storage and melting, assimilation, storage, and homogenization processes (MASH) [Hildreth and Moorbath, 1988] in the continental crust. The ABTS belt magmas form an array between primitive isotopic compositions similar to MORB (high ϵNd_i and low $^{87}\text{Sr}/^{86}\text{Sr}_i$ ratios), as observed for the Timok segment, and more evolved isotopic compositions (low ϵNd_i and high $^{87}\text{Sr}/^{86}\text{Sr}_i$ ratios), which partly overlap with the field of local Variscan granitoids as observed for the Apuseni segment. This array can be approximated by admixing of the least radiogenic sample, which presumably represents the isotopically unmodified mantle in the case of the Timok segment [Kolb et al., 2013], with varying amounts of basement granitoid. Depending on the choice of crustal assimilant, 10 to several tens of percent of crustal melt were added to the mantle-derived parental melt. Assimilation of local crustal basement is also indicated by the presence of inherited zircons in igneous rocks from most arc segments, recording Jurassic, Carboniferous, Ordovician, and older crystallization ages [Georgiev et al., 2012; Kolb et al., 2013].

The ABTS belt magmas have normal-arc as well as adakite-like geochemical signatures (Figure 4). Adakite-like signatures (La/Yb and $\text{Sr}/\text{Y} > 20$, $\text{Yb} < 1.9$ ppm, and $\text{Y} < 18$ ppm), [Defant and Drummond, 1993] are frequently associated with economic porphyry Cu-Au and epithermal Cu-Au-Mo deposits [e.g., Rohrlach and Loucks, 2005; Richards and Kerrich, 2007] but probably do not indicate slab melting as suggested in the original interpretation of adakite by Defant and Drummond [1993]. Instead, adakite-like geochemical signatures indicate plagioclase-absent fractionation of amphibole at high pressure ($> 0.8\text{--}1$ GPa and $25\text{--}30$ km) [e.g., Alonso-Perez et al., 2009] and thus reflect intermediate storage of increasingly hydrous magmas in the lower crust [Rohrlach and Loucks, 2005; Richards, 2011]. Yttrium as well as middle rare Earth elements (e.g., Sm and Dy) are preferentially incorporated into amphiboles [Davidson et al., 2007; Richards and Kerrich, 2007], and the observed increasing $(\text{La}/\text{Sm})_N$ and decreasing $(\text{Dy}/\text{Yb})_N$ ratios in magmas from all arc segments of the ABTS belt are most likely to indicate widespread hornblende fractionation (Figures 4e and 4f). Kolb et al. [2013] proposed that adakite-like signatures next to normal-arc signatures in the Timok magmas were caused by high-pressure amphibole fractionation in the lower crust, followed by variable proportions of upper crustal plagioclase fractionation (incorporating Sr) and assimilation of local basement. This interpretation might also be applicable to adakite-like rocks from the other segments of ABTS belt. We therefore conclude that all ABTS belt magmas tapped a mantle wedge source that was enriched by subduction. During ascent, the mantle magmas were modified to variable degrees by fractionation in the lower and/or the upper continental crust and varying degrees of assimilation of the local upper crust of dominantly Variscan (Late Paleozoic) age.

The ABTS belt shows pronounced across-arc age and isotopic variations during a period of 25 Myr (~ 92 to 67 Ma, Turonian to Maastrichtian). Although different segments record different periods of initiation and conclusion of arc magmatism, no major breaks in magmatic activity are observed within any of the arc segments, and all arc segments were magmatically active within a common time window of ~ 83 to ~ 75 Ma (Figure 6). Age progression in magmatic arcs away from the arc front toward the inferred subduction trench, i.e., narrowing of the arc-trench gap, is commonly interpreted in terms of progressive steepening of the subducting slab. Such steepening can be associated with slab rollback; i.e., trench migration and slab hinge retreat away from the upper

plate due to increasing slab pull forces as the age of the subducted oceanic slab increases, inducing back-arc extension in the upper plate [Heuret and Lallemand, 2005]. Trends of younging magmatic ages from paleo-north to paleo-south (that is, toward the paleo-trench), which is pronounced in the case of the Banat, Timok, and Panagyurishte segments, indicate narrowing of the arc-trench gap by up to 100 km (Figure 2), consistent with steepening of the subducting Neotethys slab and intraarc extension in the upper plate. The southward migration is particularly pronounced in the Panagyurishte segment and even more so if the plutons within the northernmost Rhodopes are included. A systematic age progression is missing in the Eastern Srednogie segment, where magmatism in a central deep marine basin (Yambol-Burgas Basin) [Georgiev et al., 2001] yields ages between 81.2 and 78.0 Ma, while older intrusions occur in the southerly adjacent region [Georgiev et al., 2012]. Magmatism in the Apuseni segment neither shows any systematic trend (or even a reversed trend?) in the age pattern. At the same time, the age range of magmatism in the Apuseni segment (75.5–80.8), as well as that of the East Srednogie segment, overlaps with magmatism in the central segments. This indicates that magmatism was relatively stationary within the upper plate during the process of subduction at both ends of ABTS belt.

Slab rollback or slab steepening also enhances corner flow within the subcontinental mantle wedge, associated with asthenospheric upwelling and partial melting [Gvirtzman and Nur, 1999]. Therefore, an increasing mantle input to the later and more southerly magmas over time, only traced by isotopic compositions in the case of the Banat and Panagyurishte segments, is in good agreement with the proposed slab steepening (Figure 6b). Many of the Apuseni magmas, however, show a distinctly higher degree of crustal contamination. In contrast to the other segments, the Timok magmas originally derived from a mantle-type source with negligible crustal contamination and show increasing crustal contamination in the younger magmas only [Kolb et al., 2013]. Locally deviating, strongly crustal-influenced isotope ratios in the Timok and Eastern Srednogie segments have been explained by a higher degree of crustal assimilation, perhaps due to thicker crust or a longer residence time in the crust relative to magmas from elsewhere in the ABTS belt [Georgiev et al., 2009b; Kolb et al., 2013].

4.2. Tectonic Significance of Comagmatic Sedimentary Basins and Shear Zones

Arc magmatism in the ABTS belt is intimately associated with Late Cretaceous sedimentary basins (Figure 2), which provide additional constraints on the state of stress in different segments of the magmatic arc. Some of them contain volcanic and volcanoclastic materials, while others lack such material. It is important to note that not all of these Late Cretaceous sedimentary basins are associated with ABTS belt magmatism. Late Cretaceous postorogenic basins unrelated to ABTS magmatism are also widespread in the Tisza and Dacia Mega-Units and are often referred to as Gosau-type basins [Willingshofer et al., 1999; Schuller et al., 2009]. They formed during collapse of overthickened and gravitationally unstable continental crust and seal former nappe contacts formed during the Early Cretaceous (“Austrian”) orogeny. Sedimentation in these older basins typically starts in Albian-Cenomanian times [Kounov and Schmid, 2013]. Only the age range of comagmatic basins (94–72 Ma) whose formation is related to ABTS magmatism rather than orogenic collapse is indicated in Figure 6.

In the northern parts of the Eastern Srednogie segment, layers of andesitic pyroclastics and reworked tephra deposits already appear in the Turonian (94–90 Ma) sedimentary sequence [Nachev and Dimitrova, 1995], but the most pronounced magmatic activity of submarine extrusive arc magmas coincides with the most intense phase of intraarc extension and crustal thinning in the Campanian 81–78 Ma [Georgiev et al., 2012]. Magmatism and sedimentation abruptly stopped

at around 72 Ma ago. The volcano-sedimentary basins east of Sofia cover the entire time span between Late Turonian and the end of Campanian (92–72 Ma) [Popov *et al.*, 2012]. Sedimentation of volcanoclastic material in the Timok segment west of Sofia starts in the Turonian and ends before the deposition of Late Campanian to Maastrichtian clastic and reefal sediments [Banješević, 2010]. These biostratigraphic constraints agree with the ~90 to 79 Ma age interval for igneous rocks associated with the volcanoclastic basin in the eastern part of the Timok segment [Kolb, 2011]. In contrast to the Eastern Srednogorie Basin, the basins in the Panagyurishte and Timok segments are marine pull-apart basins, which partly formed during dextral shearing along the Iskar-Yavoritsa shear zone [Georgiev *et al.*, 2009a; Naydenov *et al.*, 2013]. This dextral shear zone is syntectonic with felsic and mafic plutons emplaced during the 86–75 Ma time interval. Hence, pluton emplacement partly overlaps with the age span of the volcano-sedimentary parts of the Panagyurishte and Timok Basins. This suggests opening of the Panagyurishte and Timok Basins in a scenario of crustal-scale dextral strike-slip motion, interpreted in terms of dextral transpression by previous authors [Georgiev *et al.*, 2009a; Naydenov *et al.*, 2013; Georgiev *et al.*, 2014]. However, a transtensional rather than transpressional setting is indicated for two reasons: (1) the Iskar-Yavoritsa shear zone is contemporaneous with the opening of comagmatic transtensional basins [Naydenov *et al.*, 2013] and (2) the Iskar-Yavoritsa shear zone is confined to the area of deposition of the Panagyurishte and Timok Basins and has no further continuation to the east. The age of volcanoclastic sediments deposited in sedimentary basins in the Banat region is not well constrained [Barzoi and Seclaman, 2010], but magmatic dikes (76–75 Ma) are associated with Santonian-Campanian sediments (~84–72 Ma). In the Apuseni segment, moderate intraarc extension probably caused deepening within the Gosau-type orogenic collapse basins in the Campanian [Kounov and Schmid, 2013].

In summary, the onset of comagmatic sedimentation in the Late Cretaceous volcano-sedimentary basins (Figure 6) starts at ~94 Ma in the east (Eastern Srednogorie) and systematically becomes younger to the west and north (82 Ma in the Apuseni segment) and coincides with the onset of magmatic activity along the ABTS belt. This extension is therefore not related to orogenic collapse but rather to the subduction of the Neotethys Ocean triggering comagmatic basin formation along the entire continental margin of the European upper plate. Massive orthogonal intraarc extension is indicated for the Eastern Srednogorie segment, while the tectonic setting in the Panagyurishte and the Timok segments was transtensive and associated with relatively moderate extension [Georgiev *et al.*, 2009a]. Moderate extension in the peripheral Apuseni and Banat segments was of shorter duration.

4.3. Ore Deposits: Regional Stress Regime and Preservation

The regional stress regime of the crust is considered to be a critical factor in generating different styles of ore deposits. Giant porphyry Cu-Au deposits in the circum-Pacific arcs preferentially formed in arc segments that underwent contractional pulses [e.g., Sillitoe and Perelló, 2005]. Geodynamically induced horizontal compression inhibits propagation of subvertical dikes and keeps buoyant magmas trapped in sheet-like subhorizontal chambers [Tosdal and Richards, 2001; Richards, 2003; Rohrlach and Loucks, 2005]. Prolonged storage of magmas in lower crustal magma chambers is crucial for allowing enrichment in water, other volatiles, and possibly ore metals [e.g., Richards, 2003; Rohrlach and Loucks, 2005; Richards and Kerrich, 2007]. Stress relaxation eventually facilitates rapid ascent of fertile hydrous magma into the upper crust, where volatiles exsolve from the magma to form ore deposits. Magma ascent is focused in localized ascent paths such as strike-slip faults [Sillitoe and Perelló, 2005]. However, a change to strong extension is not

favorable for porphyry deposit formation, as it would result in volcanic eruption rather than magma storage in the upper crust [Tosdal and Richards, 2001; Richards, 2003].

In the Late Cretaceous ABTS arc, indications for comagmatic compression have been reported for the Panagyurishte segment [Naydenov *et al.*, 2013], but crustal-scale dextral transtension probably prevailed during the activity of the Maritsa fault system and the opening of pull-apart comagmatic basins in the Panagyurishte and Timok segments. Significant porphyry-type ore deposits occur only in these two segments, in association with magmas exhibiting adakite-like trace element characteristics [e.g., von Quadt *et al.*, 2005; Kolb *et al.*, 2013]. A near-neutral stress state of the crust with mild transtension might also explain why igneous rocks with adakite-like signatures, derived by lower crustal high-pressure amphibole fractionation, and normal-arc signatures, obtained by upper crustal assimilation and fractional crystallization, occur in spatially overlapping areas in the Timok segment [Kolb *et al.*, 2013]. The peripheral Eastern Srednogorie segment, by contrast, was under extreme extension and did not form significant porphyry-style deposits.

The NNW-SSE alignment of ore deposits in the Panagyurishte segment (between Elatsite and Elshitsa; see Figure 2) [e.g. Popov *et al.*, 2002; Moritz *et al.*, 2004] is conspicuous and was probably controlled by a deep crustal fault. The fact that the southeastern end of this linear array abuts the dextral Iskar-Yavoritsa shear zone (which itself contains synkinematic intrusions of Late Cretaceous age) [Georgiev *et al.*, 2009a] suggests that the linear Panagyurishte array may follow a tensional fault oriented parallel to the σ_1/σ_2 plane. First-rank shear zones parallel to the WNW-ESE trending Iskar-Yavoritsa shear zone and NNW-SSE tensional faults paralleling σ_1 probably focused magma ascent and fluid flow to the sites of ore deposit formation, as ore deposits in the Panagyurishte segment are primarily found along these secondary oblique and cross-arc faults [Drew, 2005; Georgiev *et al.*, 2014]. Relationships between fault zones and ore deposit formation are less evident in the Timok segment but may be obscured by more intense later tectonic overprint and poor exposure.

Partial preservation of a comparatively old porphyry Cu-Au district like the ABTS belt depends critically on limited postemplacement uplift and erosion [Groves *et al.*, 2005; Kesler and Wilkinson, 2006]. This points to postemplacement processes that prevented or counteracted substantial crustal thickening in the continental host units, which would have favored complete erosion of the volcano-sedimentary successions, as it currently happens in the Andes where preserved porphyry deposits are much younger [Sillitoe and Perelló, 2005]. Preservation of shallow volcanics in the Apuseni, Banat, and Timok segments is probably due to extensional and transtensional postemplacement processes associated with Eocene to Miocene bending around the Moesian platform and extrusion of the Carpathian-Balkan orogen into the still open Carpathian embayment [e.g., Schmid *et al.*, 1998]. Extensional tectonics followed accretion in the Aegean region from Paleogene times onwards [e.g., Burchfiel *et al.*, 2008] and resulted in core complex formation and tectonic denudation in the Rhodopes [Burg, 2011; Kaiser Rohrmeier *et al.*, 2013] (Figure 2). Extension may have also caused removal of shallow ore deposits and volcanics, and exposure of deeper crustal levels in the southern parts of the Panagyurishte and Eastern Srednogorie segments.

4.4. Reconstruction and Tectonic Model for the ABTS Belt

All reconstructions of the Carpathian-Balkan orogen are speculative to some extent due to the intense later tectonic overprint in this region [Neugebauer *et al.*, 2001; Csontos and Vörös, 2004; Stampfli and Borel, 2004; Ustaszewski *et al.*, 2008], but considering the tectonic scenario that

generated the extensive arc magmatism described in this paper provides important additional constraints. Figure 7 shows a modified paleotectonic map of the Carpathian-Balkan orogen for the Turonian (~90 Ma), indicating the Late Cretaceous position of continental blocks hosting the arc-related magmatic rocks along a gently curved magmatic arc. The reconstruction is still consistent with the block rotations proposed by *Ustaszewski et al.* [2008], but extended backward in time to indicate the location of a continuous active plate boundary at the northern margin of Neotethys, such that the observed subduction magmatism can be at least qualitatively explained.

We used the Miocene restoration by *Ustaszewski et al.* [2008] as a starting point for the reconstruction and integrated a previous retrodeformation to the Late Cretaceous situation proposed by *Fügenschuh and Schmid* [2005, their Figure 9]. Our restoration is still tentative, because exact amounts of shortening or extension and changes in the geometric configuration of the tectonic units cannot be quantified. For this new reconstruction, arc segments were rotated and translated individually, but outlines of magmatic bodies and their distribution within the segments, were left unchanged, to facilitate comparison with the present-day configuration. This is reasonable because contacts between intrusions and wall rocks are generally undeformed, indicating that displacements were concentrated along larger block faults even though these segment boundaries could rarely be defined in the field. Significant deformation within synkinematic igneous intrusions related to ABTS magmatism is directly observed only along the Iskar-Yavoritsa shear zone [*Georgiev et al.*, 2009a; *Naydenov et al.*, 2013], which was therefore used as one of the major segment boundaries in our retrodeformation.

The European foreland including Moesia is fixed in its present-day position. Paleomagnetic data provide major constraints regarding rotation when restoring the Late Cretaceous situation of the Tisza Mega-Unit of the European continental margin. Counterclockwise back rotation of the Apuseni Mountains from their respective Miocene position is required to account for the presently observed total of ~90° clockwise rotation [*Pătrașcu et al.*, 1990; *Pătrașcu et al.*, 1992; *Panaiotu*, 1998; *Marton et al.*, 2007; *van Hinsbergen et al.*, 2008]. A smaller amount of total rotation was adopted for the Banat and Timok segments for geometric reasons. Only areas to the west of an inferred link between the Maritsa fault system and the future Timok-Cerna-Jiu fault system were rotated around a rotation pole fixed to the European margin, consistent with previous restorations [e.g., *Schmid et al.*, 1998]. The Getic-Supragetic-Srednogorie Units (Dacia) and the arc segments were shifted to the south by 50 km to account for Maastrichtian and Cenozoic thrusting of the Srednogorie Unit with respect to Moesia [*Dogliani et al.*, 1996; *Banks*, 1997; *Stuart et al.*, 2011]. Our reconstruction also retrodeforms N-S extension in the Rhodopes that occurred in mid-Eocene to Miocene times [e.g., *Brun and Sokoutis*, 2007; *Burg*, 2011; *Kaiser Rohrmeier et al.*, 2013]. Measured in a N-S direction across the center of the Rhodopian core complex we restored 125 km of extension [*Brun and Sokoutis*, 2007; *van Hinsbergen and Schmid*, 2012]. This extension continuously decreases westward (see rotation model of *Brun and Sokoutis* [2007]), which results in an increase in the gap between trench and arc toward west (Figure 7). For easier comparison with Figure 2 we left the outlines of the Rhodope and Strandzha Units unchanged, being aware that substantial portions of the Rhodopes were still covered by Circum-Rhodope and Strandzha Units in the north, east, and south and by Danubian, Getic, and Serbo-Macedonian Units in the west during Late Cretaceous times. The intra-Turonian nappe stacking in the Tisza Mega-Unit [*Kounov and Schmid*, 2013] was retro-deformed by taking back 150 km of shortening. In order to achieve a better fit for the magmatic arc, the tectonic units of the Apuseni Mountains had to be shifted further to the west, compared to the restoration by *Fügenschuh and Schmid* [2005].

The width of the Neotethys remnant basin, i.e., the ocean that closed to form the Sava-Izmir-Ankara suture between Adria and Europe in the Late Cretaceous [Schmid *et al.*, 2008; Schmid *et al.*, 2011], is not well constrained and differs widely among published reconstructions [e.g., Neugebauer *et al.*, 2001; Csontos and Vörös, 2004; Stampfli and Borel, 2004]. Our interpretation of the ABTS belt as a magmatic arc above a subduction zone places an additional constraint on the minimum width of Neotethys, because a mature subduction slab must be established before arc magmatism can start. Transporting hydrated oceanic lithosphere to a typical depth required to initiate partial melting of the overriding mantle (100-120 km), and choosing the arc-trench gap of 250 km resulting from our reconstruction at 90 Ma ago, a minimum slab length of 270 km must have been subducted to trigger the onset of magmatism. This corresponds to a rather flat subduction zone with a shallow angle of 22–26°. There is considerable uncertainty on these estimates, and a shorter arc-trench gap or a higher depth of melting would result in increases or decreases in the subducted slab length, respectively, and a steeper initial subduction angle at the onset of magmatism. Given the Africa-Europe convergence rate of 15 km/Ma before 90 Ma, calculated for the N-S direction [Rosenbaum *et al.*, 2002], subduction of 270 km of oceanic lithosphere would have been initiated some 18 Ma earlier, i.e., in the Albian, which corresponds to the end of the Early Cretaceous (“Austrian”) orogeny in which the prearc nappe system along the European margin was established. An additional width of 300 km of oceanic lithosphere, remaining at 90 Ma as depicted in Figure 7, is necessary to sustain subduction-related magmatism until ~70 Ma, assuming an unchanged plate motion speed of 15 km/Ma [Rosenbaum *et al.*, 2002] until closure of the Neotethys.

The southward migration of magmatic activity within the central segments of the arc is best interpreted as resulting from a gradual increase in the subduction angle associated with a reduction of the width of the arc-trench gap. For the particularly well-documented Panagyurishte segment, 100 km of across-arc migration of magmatism from 92 to 75 Ma (67 Ma including the Rhodopes) corresponds to a steepening of the subduction angle from an initial 22–26° to 34–39° and a contraction of the arc-trench gap from an initial 250 km to 150 km. Slab rollback and southward migration of both trench and arc relative to fixed Europe is a rather unlikely alternative to explaining across-arc migration of magmatism [cf. von Quadt *et al.*, 2005], given the evidence for continued Africa-Europe convergence. Consequently, we interpret the comagmatic sedimentary basins as intraarc rift basins rather than back-arc rift basins.

The magmatic arc of the ABTS belt has natural terminations on its two ends. It terminates west of the Apuseni segment because there is no along-strike continuation of the Neotethys (Sava) Ocean, due to a change in subduction polarity between Alps and Dinarides along a transform fault that approximately coincides with the present-day mid-Hungarian shear zone (Figure 7) [Schmid *et al.*, 2008; Schmid *et al.*, 2011]. In the east the magmatic arc terminates at the West Black Sea Fault, a transform fault delimiting the oceanic Black Sea back-arc basin to the west [Okay *et al.*, 1994].

The evolution of the ABTS belt in Late Cretaceous times can be subdivided into the following three stages illustrated in Figure 8 for three representative segments of the ABTS belt:

1. *Active continental margin at ~110 Ma.* As discussed above north dipping subduction of the Neotethys Ocean along the Sava trench must have started some time before the onset of arc magmatic activity, most likely during the Albian. Sediment accumulation in subduction-related basins started between 100 and 90 Ma along the full length of the European continental margin (Figures 8a–8c). The formation of strike-slip and pull-apart basins in the Panagyurishte segment indicates that the dextral Maritsa fault system has already been

active at that time (Figure 8b). Toward the end of this stage the mantle source was geochemically enriched by subduction fluids and/or melts to generate the characteristic subduction-like signature of arc magmas. A lower crustal magma chamber, where the first magmas were further enriched in volatiles and metal content, might have already existed below the Panagyurishte and Timok segments.

2. Initiation of magmatic activity, steepening of the subduction zone, and ore deposit formation (~92 to 75 Ma). The earliest upper crustal magmatism is recorded by intrusive rocks from the northern Panagyurishte segment and indirectly by comagmatic sediments preserved in the Eastern Srednogorie segment (~92 Ma; Figures 8e and 8f). The onset of magmatic activity systematically became younger toward the west (~89 to 82 Ma; Figure 6) in the other segments of ABTS belt (Figures 6 and 8d–8f). The ascent of magmas to the upper crust might have been facilitated by the steepening of the subduction zone and was partly focused by pull-apart structures, e.g., along the Panagyurishte lineament associated with strike-slip faulting along the Maritsa fault system (Figure 8e). At the same time, magmatic activity shifted continuously to the south in all the arc segments except for the Apuseni segment, as is evidenced by progressively younger magmatic ages toward south. This age shift away from the continent toward the paleo-trench is the most compelling evidence for continuous steepening of the subduction zone, probably because of the increasing magnitude of slab pull forces. Additionally, the trend to less radiogenic, more mantle-like Sr and Nd isotope ratios in most segments and the deepening of the volcano-sedimentary basins support steepening of the subducting Neotethys slab. Economic porphyry Cu and epithermal Cu ± Au deposits coincide with early stages of magmatism in the Panagyurishte and Timok segments.

3. End of active subduction and arc magmatism by continental collision (~72 to 67 Ma). Arc magmatism within or near to the intraarc basins ceased at ~72 Ma in all the segments, but younger plutons occur further south within the Rhodopes and Strandzha Units south of the Panagyurishte and Eastern Srednogorie segments (69–67 Ma; Figures 8g and 8h). These latest plutons probably reflect the termination of active subduction of the Sava branch of Neotethys Ocean and likely mark the collision between Adria and Europe at the end of Maastrichtian (~66 Ma) [e.g., Schmid *et al.*, 2008]. Younger plutons intruded the Rhodopes only after a significant gap of some 10 Ma (55–56 Ma) [Soldatos *et al.*, 2008; Jahn-Awe *et al.*, 2010; Marchev *et al.*, 2013]. They probably intruded in a postcollisional setting after subduction in the Sava trench had stalled and the subduction zone had shifted to a new trench further south. Still younger Eocene to Oligocene (~42 to 26 Ma) magmatism in the Rhodope and Dacia Units either formed due to postcollisional slab break-off or mantle delamination [Schefer *et al.*, 2010; Marchev *et al.*, 2013] or was driven by a subduction zone now located further south in the Aegean region [Lehmann *et al.*, 2013]. Active subduction migrating southward matches a long-lived environment of slab rollback on the larger scale, progressing since the Early Cretaceous to present-day Crete, which is supported by an ~1600 km long tomographically imaged slab beneath the Aegean region [Bijwaard *et al.*, 1998; van Hinsbergen *et al.*, 2005].

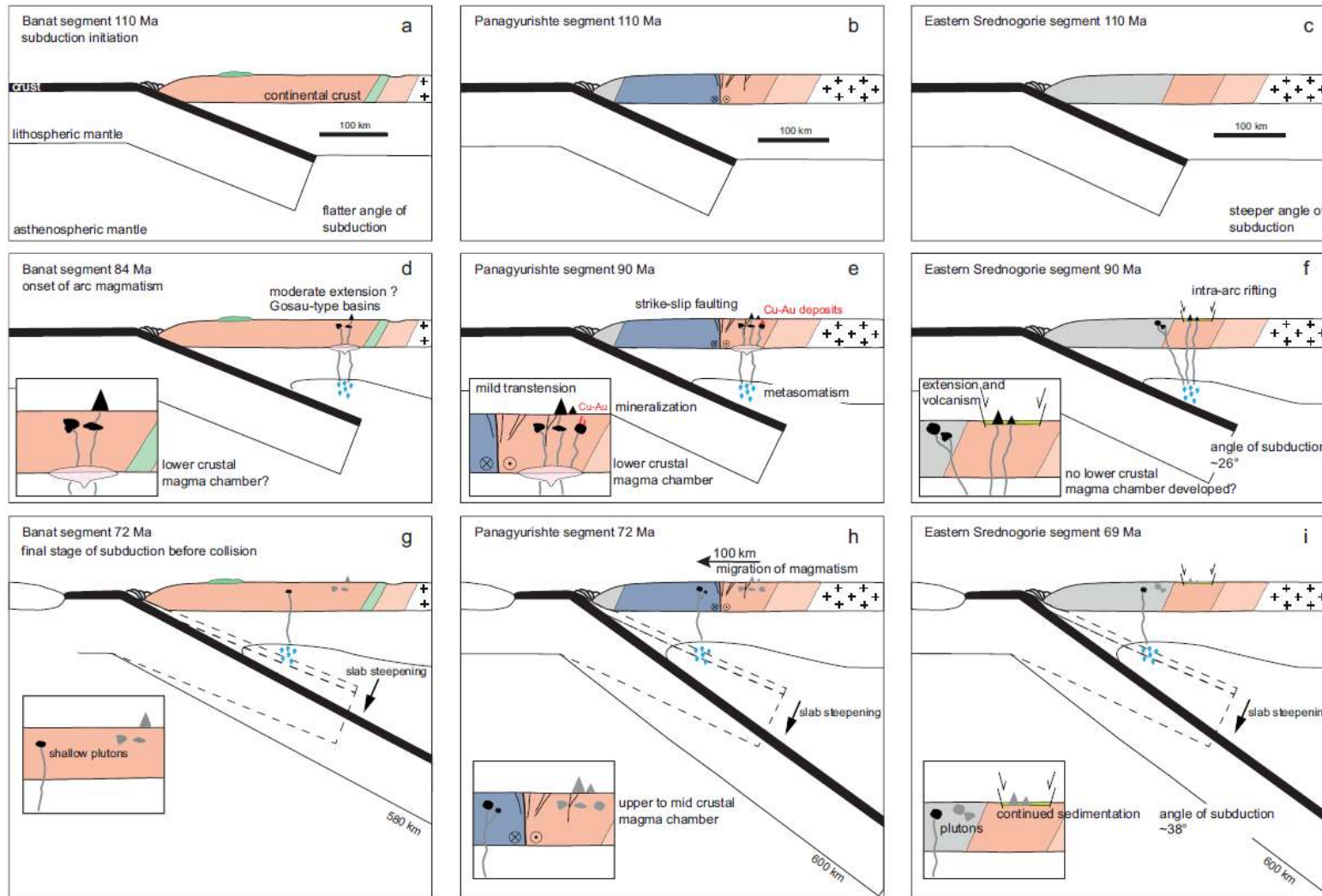


Figure 8. Schematic tectonic model for three representative segments of the ABTS belt. Late Cretaceous tectonic history of **(a, d, and g)** the Banat segment, **(b, e, and h)** the Panagyurishte segment, and **(c, f, and i)** the Eastern Srednogie segment. The colors of tectonic units are the same as in Figure 7. Blue drops = mantle source enrichment and melting, grey lines = magma ascent paths; black = active magma chambers and volcanoes; grey = extinct magma chambers and volcanoes; light green = sedimentary basins; light pink = lower crustal magma chamber. The small insets in lower left corners show a magnification of the crustal magmatic activity.

5. Summary and Conclusions

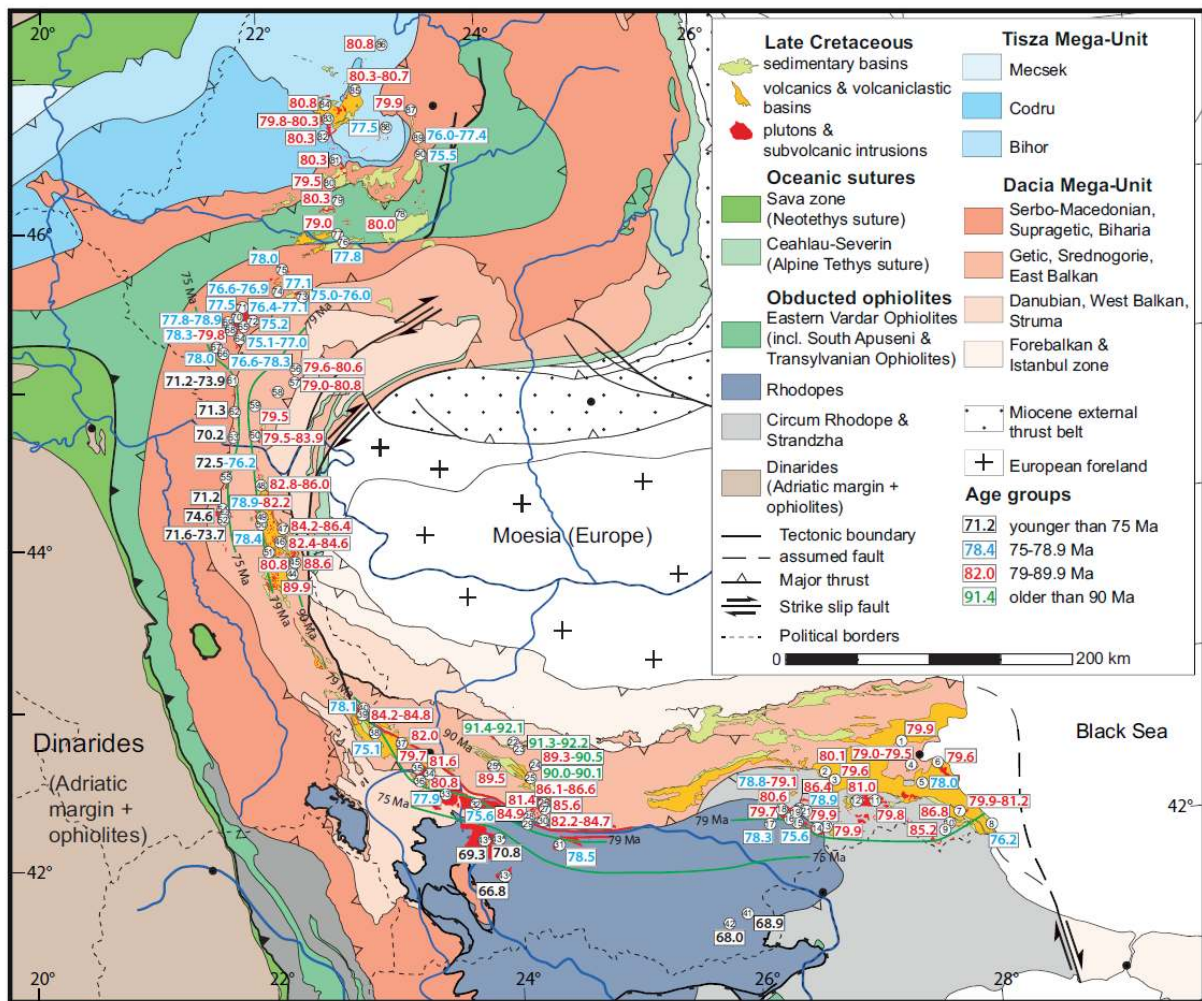
In this study we have attempted to resolve the tectonic history of the Late Cretaceous magmatic arc embedded in the Carpathian-Balkan orogen, by comparing magma-chemical signatures and age trends in distinct segments along and across the arc. Based on geochemical characteristics, the Apuseni-Banat-Timok-Srednogie (ABTS) belt can be interpreted as a typical subduction-related magmatic arc that formed on a continental margin. The arc was active for 25 Ma, and across-arc younging of the magmatic products toward the paleo-trench provides clear evidence for gradual steepening of the subducting Neotethys slab. This north to south age progression is accompanied by distinct isotopic trends in the respective arc segments, generally indicating an increasing contribution of mantle melts, which probably results from increasing asthenospheric corner flow. The contemporaneous formation of sedimentary and volcano-sedimentary basins is likely due to the same tectonic processes, i.e., subduction and slab steepening leading to intraarc extension. Economic deposits preferentially formed in the central arc segments, because these were subjected to only mild transtension during contemporaneous shearing, favoring high-pressure amphibole fractionation and accumulation of magmatic volatiles. Collision with the Adriatic plate terminated active subduction in the Sava trench and arc magmatism. Postemplacement bending of the entire arc and associated extensional tectonics partly concealed the rather simple and typical geometry of this continental magmatic arc but favored the preservation of near-surface ore deposits and shallow volcano-sedimentary basins in this relatively old metallogenic belt.

Acknowledgements

This study was supported by the Swiss National Science Foundation grants 200020-146681 and 20021-146651 and SNF scopes projects JRP 7BUPJ062396 and IZ73ZO_128089 and incorporates results by Melanie Kolb, Svetoslav Georgiev, and Majka Kaiser-Rohrmaier as early pioneers of this multi-PhD project. Ioan Seghedi provided essential help during joint field work in Romania, and we are most grateful for his regional geological insight. We thank Ramon Aubert, Markus Wälle, Marcel Guillong, Lydia Zehnder, and Muhammed Usman for their support in the laboratories. All original geochemical data used in this study, including a compilation of results from M. Kolb and S. Georgiev, are provided in digital form as supporting information. Douwe van Hinsbergen is thanked for sharing his ideas concerning plate tectonic reconstructions, influencing parts of our Figure 7. We thank Jeremy Richards and Iain Neill for their constructive reviews, which considerably improved this manuscript.

Appendix

The distribution patterns of magmatic crystallization ages can yield important additional constraints for plate tectonic reconstructions. All available magmatic ages were plotted in the present-day tectonic map (Figure A1) to identify any systematic variations of the magmatic ages along and across the magmatic arc. Pronounced across-arc variations are observed in the Panagyurishte, Timok, and Banat segments, where they change from north to south younging trends (Panagyurishte) to east to west younging trends (Timok and Banat). The rotation, which has been inferred from paleomagnetic data [e.g., Marton et al., 2007; van Hinsbergen et al., 2008], is therefore also indicated by the magmatic ages. Calculated crystallization ages for all segments are reported in Table S3. For the Banat and Apuseni segments, 2 standard deviations of overlapping and concordant TIMS or LA-ICP-MS ages in a population of analyses of each sample are reported, as a conservative measure of age uncertainty, rather than standard errors of the mean that become unrealistically small in the case of numerous point analyses.



Appendix Figure A1: Tectonic map of the ABTS belt summarizing the crystallization ages of the magmatic rocks. Numbers in zircons correspond to numbering of occurrences in Table S3. LA-ICP-MS and TIMS single zircon dates and Concordia plots for the Banat and Apuseni segments are provided in Tables S4 and S5 and Figure S1.

Cited References

Alonso-Perez, R., O. Müntener, and P. Ulmer (2009), Igneous garnet and amphibole fractionation in the roots of island arcs: experimental constraints on andesitic liquids, *Contrib. Mineral. Petrol.*, 157(4), 541-558, doi: 10.1007/s00410-008-0351-8.

Annen, C., J. D. Blundy, and R. S. J. Sparks (2006), The genesis of intermediate and silicic magmas in deep crustal hot zones, *J. Petrol.*, 47(3), 505-539.

Atanasova-Vladimirova, S., A. von Quadt, P. Marchev, I. Peytcheva, I. Piroeva, and B. Mavrudchiev (2010), Petrology and geochronology of the Vitoshka volcano-plutonic edifice, Western Srednogie, Bulgaria, *Geologica Balcanica*, 39(1-2), 31-32.

Balla, Z. (1987), Tertiary palaeomagnetic data for the Carpatho-Pannonian region in the light of Miocene rotation kinematics, *Tectonophysics*, 139(1-2), 67-98, doi: dx.doi.org/10.1016/0040-1951(87)90198-3.

Banješević, M. (2010), Upper Cretaceous magmatic suites of the Timok Magmatic Complex, *Annales Géologiques de la Péninsule Balkanique*, 71, 13-22.

Banks, C. J. (1997), Basins and thrust belts of the Balkan Coast of the Black Sea, *Regional and Petroleum Geology of the Black Sea and Surrounding Region*, 68, 115-128.

Barzoi, S. C., and M. Seclaman (2010), Petrographic and geochemical interpretation of the Late Cretaceous volcanoclastic deposits from the Hateg Basin, *Palaeogeography, Palaeoclimatology, Palaeoecology*, 293(3-4), 306-318, doi: 10.1016/j.palaeo.2009.08.028.

Berza, T., E. Constantinescu, and S. N. Vlad (1998), Upper Cretaceous Magmatic Series and Associated Mineralisation in the Carpathian – Balkan Orogen, *Resource Geology*, 48(4), 291-306, doi: 10.1111/j.1751-3928.1998.tb00026.x.

Bidzhova, L., R. Nedialkov, M. Ovtcharova, and A. von Quadt (2013), Precise U-Pb zircon CA-ID-TIMS ages and Sr isotopes for the Plana pluton, Srednogie, Bulgaria, *Mineralogical Magazine*, 77(55), 704.

Bijwaard, H., W. Spakman, and E. R. Engdahl (1998), Closing the gap between regional and global travel time tomography, *Journal of Geophysical Research: Solid Earth*, 103(B12), 30055-30078, doi: 10.1029/98JB02467.

Boccaletti, M., P. Manetti, and Pecceril, A. (1974), Hypothesis on the plate tectonic evolution of the Carpatho-Balkan Arcs, *Earth Planet. Sci. Lett.*, 23(2), 193-198, doi: 10.1016/0012-821x(74)90193-9.

Bonev, N., and G. Stampfli (2011), Alpine tectonic evolution of a Jurassic subduction-accretionary complex: Deformation, kinematics and $^{40}\text{Ar}/^{39}\text{Ar}$ age constraints on the Mesozoic low-grade schists of the Circum-Rhodope Belt in the eastern Rhodope-Thrace region, Bulgaria-Greece, *Journal of Geodynamics*, 52(2), 143-167, doi: dx.doi.org/10.1016/j.jog.2010.12.006.

Bonev, N., J. P. Burg, and Z. Ivanov (2006), Mesozoic-Tertiary structural evolution of an extensional gneiss dome - the Kesebir-Kardamos dome, eastern Rhodope (Bulgaria-Greece), *Int. J. Earth Sci.*, 95(2), 318-340, doi: 10.1007/s00531-005-0025-y.

Bouilhol, P., O. Jagoutz, J. M. Hanchar, and F. O. Dudas (2013), Dating the India-Eurasia collision through arc magmatic records, *Earth Planet. Sci. Lett.*, 366, 163-175, doi: 10.1016/j.epsl.2013.01.023.

Brun, J.-P., and D. Sokoutis (2007), Kinematics of the Southern Rhodope Core Complex (North Greece), *Int. J. Earth Sci.*, 96(6), 1079-1099, doi: 10.1007/s00531-007-0174-2.

Burchfiel, B. C., R. Nakov, N. Dumurdzanov, D. Papanikolaou, T. Tzankov, T. Serafimovski, R. W. King, V. Kotzev, A. Todosov, and B. Nurce (2008), Evolution and dynamics of the Cenozoic tectonics of the South Balkan extensional system, *Geosphere*, 4(6), 919-938, doi: 10.1130/ges00169.1.

Burg, J.-P. (2011), Rhodope: From Mesozoic convergence to Cenozoic extension. Review of petro-structural data in the geochronological frame, *Journal of the Virtual Explorer*, 39(1), 44.

Burnham, C. W. (1979), Magmas and hydrothermal fluids, in *Geochemistry of hydrothermal ore deposits*, edited by H. L. Barnes, pp. 71-136, John Wiley and Sons, New York.

Camus, F. (2002), The Andean porphyry systems, in *Centre for Ore Deposit Research Special Publication*, edited, pp. 5-22, University of Tasmania.

Chambefort, I., R. Moritz, and A. von Quadt (2007), Petrology, geochemistry and U-Pb geochronology of magmatic rocks from the high-sulfidation epithermal Au-Cu Chelopech deposit, Srednogorie zone, Bulgaria, *Miner. Depos.*, 42(7), 665-690, doi: 10.1007/s00126-007-0126-6.

Chiaradia, M. (2009), Adakite-like magmas from fractional crystallization and melting-assimilation of mafic lower crust (Eocene Macuchi arc, Western Cordillera, Ecuador), *Chem. Geol.*, 265(3-4), 468-487, doi: 10.1016/j.chemgeo.2009.05.014.

Ciobanu, C., N. Cook, and H. Stein (2002), Regional setting and geochronology of the Late Cretaceous Banatitic Magmatic and Metallogenic Belt, *Miner. Depos.*, 37(6), 541-567, doi: 10.1007/s00126-002-0272-9.

Cooke, D. R., P. Hollings, and J. L. Walsh (2005), Giant porphyry deposits: Characteristics, distribution, and tectonic controls, *Econ. Geol.*, 100(5), 801-818, doi: 10.2113/100.5.801.

Cross, T. A., and R. H. Pilger (1982), Controls of subduction geometry, location of magmatic arcs, and tectonics of arc and back-arc regions, *Geol. Soc. Am. Bull.*, 93(6), 545-562, doi: 10.1130/0016-7606(1982)93<545:cosglo>2.0.co;2.

Csontos, L., and A. Vörös (2004), Mesozoic plate tectonic reconstruction of the Carpathian region, *Palaeogeography, Palaeoclimatology, Palaeoecology*, 210(1), 1-56, doi: 10.1016/j.palaeo.2004.02.033.

Dallmeyer, R. D., D. I. Pana, F. Neubauer, and P. Erdmer (1999), Tectonothermal evolution of the Apuseni Mountains, Romania: Resolution of Variscan versus alpine events with Ar-40/Ar-39 ages, *Journal of Geology*, 107(3), 329-352, doi: 10.1086/314352.

Dallmeyer, R. D., F. Neubauer, R. Handler, H. Fritz, W. Muller, D. Pana, and M. Putis (1996), Tectonothermal evolution of the internal Alps and Carpathians: Evidence from Ar-40/Ar-39 mineral and whole-rock data, *Eclogae Geologicae Helveticae*, 89(1), 203-227.

Davidson, J., S. Turner, H. Handley, C. Macpherson, and A. Dosseto (2007), Amphibole "sponge" in arc crust?, *Geology*, 35(9), 787-790, doi: 10.1130/g23637a.1.

Davies, J. H., and F. von Blanckenburg (1995), Slab breakoff: A model of lithosphere detachment and its test in the magmatism and deformation of collisional orogens, *Earth Planet. Sci. Lett.*, 129(1-4), 85-102, doi: 10.1016/0012-821X(94)00237-S.

de Boorder, H., W. Spakman, S. H. White, and M. J. R. Wortel (1998), Late Cenozoic mineralization, orogenic collapse and slab detachment in the European Alpine Belt, *Earth Planet. Sci. Lett.*, 164(3-4), 569-575, doi: 10.1016/S0012-821X(98)00247-7.

de Paolo, D. J. (1981), Trace-element and isotopic effects of combined wallrock assimilation and fractional crystallization, *Earth Planet. Sci. Lett.*, 53(2), 189-202, doi: 10.1016/0012-821x(81)90153-9.

Defant, M. J., and M. S. Drummond (1993), Mount St. Helens - Potential example of the partial melting of the subducted lithosphere in a volcanic arc, *Geology*, 21(6), 547-550, doi: 10.1130/0091-7613(1993)021<0547:mshpeo>2.3.co;2.

Dewey, J. F., W. C. Pitman, W. B. F. Ryan, and J. Bonnin (1973), Plate Tectonics and the Evolution of the Alpine System, *Geol. Soc. Am. Bull.*, 84(10), 3137-3180, doi: 10.1130/0016-7606(1973)84<3137:ptateo>2.0.co;2.

Dogliani, C., C. Busatta, G. Bolis, L. Marianini, and M. Zanella (1996), Structural evolution of the eastern Balkans (Bulgaria), *Marine and Petroleum Geology*, 13(2), 225-251, doi: 10.1016/0264-8172(95)00045-3.

Drew, L. J. (2005), A tectonic model for the spatial occurrence of porphyry copper and polymetallic vein deposits: applications to central Europe *Rep.*, 36 pp, USGS, Reston.

Duchesne, J.-C., J.-P. Liègeois, V. Iancu, T. Berza, D. Matukov, M. Tatu, and S. Sergeev (2008), Post-collisional melting of crustal sources: constraints from geochronology, petrology and Sr, Nd isotope geochemistry of the Variscan Sichevita and Poniasca granitoid plutons (South Carpathians, Romania), *Int. J. Earth Sci.*, 97(4), 705-723, doi: 10.1007/s00531-007-0185-z.

Elliott, T. (2003), Tracers of the slab, *Geophysical Monograph Series*, 138, 23-45.

Fillerup, M. A., J. H. Knapp, C. C. Knapp, and V. Raileanu (2010), Mantle earthquakes in the absence of subduction? Continental delamination in the Romanian Carpathians, *Lithosphere*, 2(5), 333-340, doi: 10.1130/l102.1.

Fügenschuh, B., and S. M. Schmid (2005), Age and significance of core complex formation in a very curved orogen: Evidence from fission track studies in the South Carpathians (Romania), *Tectonophysics*, 404(1-2), 33-53, doi: 10.1016/j.tecto.2005.03.019.

Garwin, S., R. Hall, and Y. Watanabe (2005), Tectonic Setting, Geology, and Gold and Copper Mineralization in Cenozoic Magmatic Arcs of Southeast Asia and the West Pacific, *Econ. Geol.*, 100th Anniversary Volume, 891-930.

Georgiev, G., C. Dabovski, and G. Stanisheva-Vassileva (2001), East Srednogorie-Balkan Rift Zone, in *Peri-Tethys Memoir 6: Peri-Tethyan Rift/Wrench Basins and Passive Margins*, edited by P. A. Ziegler, W. Cavazza, A. H. F. Robertson and S. CrasquinSoleau, pp. 259-293, Publications Scientifiques Du Museum, Paris.

Georgiev, N., B. Henry, N. Jordanova, D. Jordanova, and K. Naydenov (2014), Emplacement and fabric-forming conditions of plutons from structural and magnetic fabric analysis: A case study of the Plana pluton (Central Bulgaria), *Tectonophysics*, 629(0), 138-154, doi: 10.1016/j.tecto.2014.02.018.

Georgiev, N., B. Henry, N. Jordanova, N. Froitzheim, D. Jordanova, Z. Ivanov, and D. Dimov (2009a), The emplacement mode of Upper Cretaceous plutons from the southwestern part of the Sredna Gora Zone (Bulgaria) structural and AMS study, *Geologica Carpathica*, 60(1), 15-33, doi: 10.2478/v10096-009-0001-8.

Georgiev, S., A. von Quadt, C. A. Heinrich, I. Peytcheva, and P. Marchev (2012), Time evolution of a rifted continental arc: Integrated ID-TIMS and LA-ICPMS study of magmatic zircons from the Eastern Srednogorie, Bulgaria, *Lithos*, 154(0), 53-67, doi: 10.1016/j.lithos.2012.06.020.

Georgiev, S., P. Marchev, C. A. Heinrich, A. Von Quadt, I. Peytcheva, and P. Manetti (2009b), Origin of Nepheline-normative High-K Ankarmites and the Evolution of Eastern Srednogie Arc in SE Europe, *J. Petrol.*, 50(10), 1899-1933, doi: 10.1093/petrology/egp056.

Görür, N. (1988), Timing of opening of the Black Sea basin, *Tectonophysics*, 147(3-4), 247-262, doi: 10.1016/0040-1951(88)90189-8.

Groves, D. I., and F. P. Bierlein (2007), Geodynamic settings of mineral deposit systems, *Journal of the Geological Society*, 164(1), 19-30, doi: 10.1144/0016-76492006-065.

Groves, D. I., R. M. Vielreicher, R. J. Goldfarb, and K. C. Condie (2005), Controls on the heterogeneous distribution of mineral deposits through time, *Geological Society, London, Special Publications*, 248(1), 71-101, doi: 10.1144/gsl.sp.2005.248.01.04.

Gvirtzman, Z., and A. Nur (1999), Plate detachment, asthenosphere upwelling, and topography across subduction zones, *Geology*, 27(6), 563-566, doi: 10.1130/0091-7613(1999)027<0563:pdauat>2.3.co;2.

Haas, J., and C. Pero (2004), Mesozoic evolution of the Tisza Mega-unit, *Int. J. Earth Sci.*, 93(2), 297-313, doi: 10.1007/s00531-004-0384-9.

Handy, M. R., S. M. Schmid, R. Bousquet, E. Kissling, and D. Bernoulli (2010), Reconciling plate-tectonic reconstructions of Alpine Tethys with the geological-geophysical record of spreading and subduction in the Alps, *Earth-Science Reviews*, 102(3-4), 121-158, doi: 10.1016/j.earscirev.2010.06.002.

Harangi, S., and L. Lenkey (2007), Genesis of the Neogene to Quaternary volcanism in the Carpathian-Pannonian region: Role of subduction, extension, and mantle plume, *Geological Society of America Special Papers*, 418, 67-92, doi: 10.1130/2007.2418(04).

Haschke, M. R., E. Scheuber, A. Günther, and K. J. Reutter (2002), Evolutionary cycles during the Andean orogeny: repeated slab breakoff and flat subduction?, *Terra Nova*, 14(1), 49-55, doi: 10.1046/j.1365-3121.2002.00387.x.

Heinrich, C. A., and F. Neubauer (2002), Cu-Au-Pb-Zn-Ag metallogeny of the Alpine-Balkan-Carpathian-Dinaride geodynamic province, *Miner. Depos.*, 37(6-7), 533-540, doi: 10.1007/s00126-002-0271-x.

Herz, N., and H. Savu (1974), Plate tectonics history of Romania, *Geol. Soc. Am. Bull.*, 85(9), 1429-1440, doi: 10.1130/0016-7606(1974)85<1429:pthor>2.0.co;2.

Heuret, A., and S. Lallemand (2005), Plate motions, slab dynamics and back-arc deformation, *Phys. Earth Planet. Inter.*, 149(1-2), 31-51, doi: 10.1016/j.pepi.2004.08.022.

Hildreth, W., and S. Moorbath (1988), Crustal contributions to arc magmatism in the Andes of Central Chile, *Contrib. Mineral. Petrol.*, 98(4), 455-489, doi: 10.1007/bf00372365.

Iancu, V., T. Berza, A. Seghedi, I. Gheuca, and H.-P. Hann (2005), Alpine polyphase tectono-metamorphic evolution of the South Carpathians: A new overview, *Tectonophysics*, 410(1-4), 337-365, doi: 10.1016/j.tecto.2004.12.038.

Irvine, T. N., and W. R. A. Baragar (1971), Guide to chemical classification of common volcanic rocks, *Canadian Journal of Earth Sciences*, 8(5), 523-548, doi: 10.1139/e71-055.

Jahn-Awe, S., N. Froitzheim, T. J. Nagel, D. Frei, N. Georgiev, and J. Pleuger (2010), Structural and geochronological evidence for Paleogene thrusting in the western Rhodopes, SW Bulgaria: Elements for a new tectonic model of the Rhodope Metamorphic Province, *Tectonics*, 29, doi: 10.1029/2009tc002558.

Jankovic, S. (1997), The Carpatho-Balkanides and adjacent area: a sector of the Tethyan Eurasian metallogenic belt, *Miner. Depos.*, 32(5), 426-433, doi: 10.1007/s001260050110.

Kaiser Rohrmeier, M., A. von Quadt, T. Driesner, C. A. Heinrich, R. Handler, M. Ovtcharova, Z. Ivanov, P. Petrov, S. St. and I. Peytcheva (2013), Post-Orogenic Extension and Hydrothermal Ore Formation: High-Precision Geochronology of the Central Rhodopian Metamorphic Core Complex (Bulgaria-Greece), *Econ. Geol.*, 108(4), 691-718.

Kamenov, B. K., A. von Quadt, and I. Peytcheva (2003), Capitan-Dimitriev pluton in Central Srednogorie, Bulgaria: Mineral chemistry, geochemistry and isotope evidence for magma-mixing origin, *Geochemistry, Mineralogy and Petrology*, 40, 21-53.

Kamenov, B. K., Y. Yanev, R. Nedialkov, R. Moritz, I. Peytcheva, A. von Quadt, S. Stoykov, and A. Zartova (2007), Petrology of Upper Cretaceous island-arc ore-magmatic centers from Central Srednogorie, Bulgaria: Magma evolution and paths, *Geochemistry, Mineralogy and Petrology*, 45, 39-77.

Karamata, S. (2006), The geological development of the Balkan Peninsula related to the approach, collision and compression of Gondwanan and Eurasian units, *Geological Society, London, Special Publications*, 260(1), 155-178, doi: 10.1144/gsl.sp.2006.260.01.07.

Kay, S. M., and B. L. Coira (2009), Shallowing and steepening subduction zones, continental lithospheric loss, magmatism, and crustal flow under the Central Andean Altiplano-Puna Plateau, *Geol. Soc. Am. Mem.*, 204, 229-259, doi: 10.1130/2009.1204(11).

Kay, S. M., C. Mpodozis, and B. Coira (1999), Neogene magmatism, tectonism, and mineral deposits of the Central Andes (22 to 33 S latitude), *Geology and Ore Deposits of the Central Andes (Skinner, B); editor. Society of Economic Geologists, Special Publication*, 7, 27-59.

Kesler, S. E., and B. H. Wilkinson (2006), The role of exhumation in the temporal distribution of ore deposits, *Econ. Geol.*, 101(5), 919-922, doi: 10.2113/gsecongeo.101.5.919.

Kolb, M. (2011), Geochronology and isotope geochemistry of magmatic rocks from Western Srednogorie (Bulgaria) and Timok Magmatic Complex (East Serbia), PhD thesis, 173 pp, ETH Zurich, Zurich.

Kolb, M., A. Von Quadt, I. Peytcheva, C. A. Heinrich, S. J. Fowler, and V. Cvetkovic (2013), Adakite-like and Normal Arc Magmas: Distinct Fractionation Paths in the East Serbian Segment of the Balkan-Carpathian Arc, *J. Petrol.*, 54(3), 421-451, doi: 10.1093/petrology/egs072.

Kounov, A., and S. M. Schmid (2013), Fission-track constraints on the thermal and tectonic evolution of the Apuseni Mountains (Romania), *Int. J. Earth Sci.*, 102(1), 207-233, doi: 10.1007/s00531-012-0800-5.

Kounov, A., D. Seward, J. P. Burg, D. Bernoulli, Z. Ivanov, and R. Handler (2010), Geochronological and structural constraints on the Cretaceous thermotectonic evolution of the Kraishte zone, western Bulgaria, *Tectonics*, 29, doi: 10.1029/2009tc002509.

Kouzmanov, K., R. Moritz, A. von Quadt, M. Chiaradia, I. Peytcheva, D. Fontignie, C. Ramboz, and K. Bogdanov (2009), Late Cretaceous porphyry Cu and epithermal Cu–Au association in the Southern Panagyurishte District, Bulgaria: the paired Vlaykov Vruh and Elshitsa deposits, *Miner. Depos.*, 44(6), 611-646, doi: 10.1007/s00126-009-0239-1.

Kräutner, H. G., and B. Krstić (2002), *Alpine and Pre-Alpine structural Units within the Southern Carpathians and the Western Balkanides.*, Bratislava.

Kräutner, H. G., and B. Krstić (2003), *Geological map of the Carpatho-Balkanides between Mehadia, Oravita, Nis and Sofia.*, Geoinstitut, Belgrade.

Krenn, K., C. Bauer, A. Proyer, U. Klötzli, and G. Hoinkes (2010), Tectonometamorphic evolution of the Rhodope orogen, *Tectonics*, 29(4), TC4001, doi: 10.1029/2009TC002513.

Kuno, H. (1968), *Differentiation of basaltic magmas*, John Wiley & Sons, New York.

Lang, J. R., and S. R. Titley (1998), Isotopic and geochemical characteristics of Laramide magmatic systems in Arizona and implications for the genesis of porphyry copper deposits, *Econ. Geol.*, 93(2), 138-170, doi: 10.2113/gsecongeol.93.2.138.

Le Maitre, R. W., et al. (1989), *A classification of igneous rocks and glossary of terms*, 191 pp., Blackwell, Oxford.

Lehmann, S., J. Barcikowski, A. von Quadt, D. Gallhofer, I. Peytcheva, C. A. Heinrich, and T. Serafimovski (2013), Geochronology, geochemistry and isotope tracing of the Oligocene magmatism of the Buchim–Damjan–Borov Dol ore district: Implications for timing, duration and source of the magmatism, *Lithos*, 180–181(0), 216-233, doi: 10.1016/j.lithos.2013.09.002.

Loucks, R. R. (2014), Distinctive composition of copper-ore-forming arc magmas, *Australian Journal of Earth Sciences*, 61(1), 5-16, doi: 10.1080/08120099.2013.865676.

Mahlburg Kay, S., R. W. Kay, and G. P. Citron (1982), Tectonic controls on tholeiitic and calc-alkaline magmatism in the Aleutian Arc, *Journal of Geophysical Research: Solid Earth*, 87(B5), 4051-4072, doi: 10.1029/JB087iB05p04051.

Marchev, P., A. von Quadt, I. Peytcheva, and M. Ovtcharova (2006), The age and origin of the Chuchuliga and Rozino granites, Eastern Rhodopes, paper presented at Geosciences, Bulgarian Geological Society, Sofia, Bulgaria.

Marchev, P., S. Georgiev, R. Raicheva, I. Peytcheva, A. von Quadt, M. Ovtcharova, and N. Bonev (2013), Adakitic magmatism in post-collisional setting: An example from the Early–Middle Eocene Magmatic Belt in Southern Bulgaria and Northern Greece, *Lithos*, 180–181(0), 159-180, doi: 10.1016/j.lithos.2013.08.024.

Marton, E., M. Tischler, L. Csontos, B. Fuegenschuh, and S. M. Schmid (2007), The contact zone between the ALCAPA and Tisza-Dacia megatectonic units of Northern Romania in the light of new paleomagnetic data, *Swiss Journal of Geosciences*, 100(1), 109-124, doi: 10.1007/s00015-007-1205-5.

Marton, E., D. Zampieri, P. Grandesso, V. Cosovic, and A. Moro (2010), New Cretaceous paleomagnetic results from the foreland of the Southern Alps and the refined apparent polar wander path for stable Adria, *Tectonophysics*, 480(1-4), 57-72, doi: 10.1016/j.tecto.2009.09.003.

Matenco, L., C. Krézsek, S. Merten, S. Schmid, S. Cloetingh, and P. Andriessen (2010), Characteristics of collisional orogens with low topographic build-up: an example from the Carpathians, *Terra Nova*, 22(3), 155-165, doi: 10.1111/j.1365-3121.2010.00931.x.

Morelli, A., and E. Barrier (2004), Geodynamic map of the Mediterranean, sheet 2, Paris.

Moritz, R., K. Kouzmanov, and R. Petrunov (2004), Late Cretaceous Cu-Au epithermal deposits of the Panagyurishte district, Srednogorie zone, Bulgaria, *Schweiz. Mineral. Petrogr. Mitt.*, 84(1-2), 79-99.

Nachev, I., and E. Dimitrova (1995), Upper Cretaceous stratigraphy of the Eastern Sredna Gora zone, *Geologica Balcanica*, 25, 3-26.

Naydenov, K., I. Peytcheva, A. von Quadt, S. Sarov, K. Kolcheva, and D. Dimov (2013), The Maritsa strike-slip shear zone between Kostenets and Krichim towns, South Bulgaria - Structural, petrographic and isotope geochronology study, *Tectonophysics*, 595, 69-89, doi: 10.1016/j.tecto.2012.08.005.

Nedkova, K., N. Petrov, and I. Peytcheva (2012), Age of the porphyritic intrusions from Golyama Rakovitsa ore occurrence, paper presented at Geosciences, Bulgarian Geological Society, Sofia, Bulgaria.

Neubauer, F. (2002), Contrasting Late Cretaceous with Neogene ore provinces in the Alpine-Balkan-Carpathian-Dinaride collision belt, in *Timing and Location of Major Ore Deposits in an Evolving Orogen*, edited by D. J. N. F. V. A. Blundell, pp. 81-102.

Neugebauer, J., B. Greiner, and E. Appel (2001), Kinematics of the Alpine-West Carpathian orogen and palaeogeographic implications, *Journal of the Geological Society*, 158, 97-110.

Okay, A. I., A. M. Celal Şengör, and N. Görür (1994), Kinematic history of the opening of the Black Sea and its effect on the surrounding regions, *Geology*, 22(3), 267-270, doi: 10.1130/0091-7613(1994)022<0267:khotoo>2.3.co;2.

Okay, A. I., M. Satir, O. Tuysuz, S. Akyuz, and F. Chen (2001), The tectonics of the Strandja Massif: late-Variscan and mid-Mesozoic deformation and metamorphism in the northern Aegean, *Int. J. Earth Sci.*, 90(2), 217-233.

Pamic, J. (2002), The Sava-varadar Zone of the Dinarides and Hellenides versus the Vardar Ocean, *Eclogae Geologicae Helveticae*, 95(1), 99-113.

Panaiotu, C. (1998), Paleomagnetic constraints on the geodynamic history of Romania, *Monograph of Southern Carpathians. Reports on Geodesy*, 7(37), 205-216.

Pătraşcu, S., M. Bleahu, and C. Panaiotu (1990), Tectonic implications of paleomagnetic research into Upper Cretaceous magmatic rocks in the Apuseni Mountains, Romania, *Tectonophysics*, 180(2-4), 309-322, doi: 10.1016/0040-1951(90)90316-z.

Pătrașcu, S., M. Bleahu, C. Panaiotu, and C. E. Panaiotu (1992), The paleomagnetism of the Upper Cretaceous magmatic rocks in the Banat area of South Carpathians: tectonic implications, *Tectonophysics*, 213(3-4), 341-352, doi: 10.1016/0040-1951(92)90462-f.

Perelló, J., A. Raziq, J. Schloderer, and R. Asad Ur (2008), The Chagai Porphyry Copper Belt, Baluchistan Province, Pakistan, *Econ. Geol.*, 103(8), 1583-1612.

Peytcheva, I., A. von Quadt, K. Naydenov, S. Sarov, D. Dimov, and E. Voinova (2007), U-Pb zircon-xenotime-monazite dating and Hf-isotope tracing to distinguish Cretaceous and Paleogene granitoids in the Western Rhodopes and Rila Mountain, paper presented at Geosciences, Bulgarian Geological Society, Sofia, Bulgaria.

Peytcheva, I., A. von Quadt, N. Georgiev, Z. Ivanov, C. A. Heinrich, and M. Frank (2008), Combining trace-element compositions, U-Pb geochronology and Hf isotopes in zircons to unravel complex calcalkaline magma chambers in the Upper Cretaceous Srednogorie zone (Bulgaria), *Lithos*, 104(1-4), 405-427, doi: 10.1016/j.lithos.2008.01.004.

Peytcheva, I., A. von Quadt, F. Neubauer, M. Frank, R. Nedialkov, C. A. Heinrich, and S. Strashimirov (2009), U-Pb dating, Hf-isotope characteristics and trace-REE-patterns of zircons from Medet porphyry copper deposit, Bulgaria: implications for timing, duration and sources of ore-bearing magmatism, *Mineralogy and Petrology*, 96(1), 19-41, doi: 10.1007/s00710-009-0042-9.

Popov, P., T. Berza, A. Grubic, and D. Ioane (2002), Late Cretaceous Apuseni-Banat-Timok-Srednogorie (ABTS) Magmatic and Metallogenic belt in the Carpathian-Balkan orogen, *Geologica Balcanica*, 32(2-4), 145-163.

Popov, P., S. Strashimirov, K. Popov, K. Bogdanov, R. Radichev, S. Dimovski, and S. Stoykov (2012), *Geology and metallogeny of the Panagyurishte ore region*, 227 pp., Ivan Rilski Publishing House, Sofia.

Prelevic, D., S. F. Foley, R. Romer, and S. Conticelli (2008), Mediterranean tertiary lamproites derived from multiple source components in postcollisional geodynamics, *Geochimica Et Cosmochimica Acta*, 72(8), 2125-2156, doi: 10.1016/j.gca.2008.01.029.

Ramos, V. A., and A. Folguera (2009), Andean flat-slab subduction through time, *Geological Society, London, Special Publications*, 327(1), 31-54, doi: 10.1144/sp327.3.

Ratschbacher, L., H. G. Linzer, F. Moser, R. O. Strusievicz, H. Bedelea, N. Har, and P. A. Mogos (1993), Cretaceous to Miocene thrusting and wrenching along the Central South Carpathians due to a corner effect during collision and orocline formation, *Tectonics*, 12(4), 855-873, doi: 10.1029/93tc00232.

Rice, S. P., A. H. F. Robertson, T. Ustaömer, N. İnan, and K. Tasli (2009), Late Cretaceous–Early Eocene tectonic development of the Tethyan suture zone in the Erzincan area, Eastern Pontides, Turkey, *Geological Magazine*, 146(04), 567-590, doi: 10.1017/S0016756809006360.

Richards, J. P. (2003), Tectono-magmatic precursors for porphyry Cu-(Mo-Au) deposit formation, *Econ. Geol. Bull. Soc. Econ. Geol.*, 98(8), 1515-1533, doi: 10.2113/98.8.1515.

Richards, J. P. (2011), High Sr/Y arc magmas and porphyry Cu ± Mo ± Au deposits: Just add water, *Econ. Geol.*, 106(7), 1075-1081, doi: 10.2113/econgeo.106.7.1075.

Richards, J. P. (2015), Tectonic, magmatic, and metallogenic evolution of the Tethyan orogen: From subduction to collision, *Ore Geology Reviews*(0), doi: <http://dx.doi.org/10.1016/j.oregeorev.2014.11.009>.

Richards, J. P., and R. Kerrich (2007), Special paper: Adakite-like rocks: Their diverse origins and questionable role in metallogenesis, *Econ. Geol.*, 102(4), 537-576, doi: 10.2113/gsecongeo.102.4.537.

Richards, J. P., A. J. Boyce, and M. S. Pringle (2001), Geologic Evolution of the Escondida Area, Northern Chile: A Model for Spatial and Temporal Localization of Porphyry Cu Mineralization, *Econ. Geol.*, 96(2), 271-305, doi: 10.2113/gsecongeo.96.2.271.

Richards, J. P., T. Spell, E. Rameh, A. Razique, and T. Fletcher (2012), High Sr/Y Magmas Reflect Arc Maturity, High Magmatic Water Content, and Porphyry Cu +/- Mo +/- Au Potential: Examples from the Tethyan Arcs of Central and Eastern Iran and Western Pakistan, *Econ. Geol.*, 107(2), 295-332.

Rickwood, P. C. (1989), Boundary lines within petrologic diagrams which use oxides of major and minor elements, *Lithos*, 22(4), 247-263, doi: 10.1016/0024-4937(89)90028-5.

Ricou, L. E., J. P. Burg, I. Godfriaux, and Z. Ivanov (1998), Rhodope and vardar: the metamorphic and the olistostromic paired belts related to the Cretaceous subduction under Europe, *Geodinamica Acta*, 11(6), 285-309, doi: 10.1016/s0985-3111(99)80018-7.

Rohrlach, B. D., and R. R. Loucks (2005), *Multi-million-year cyclic ramp-up of volatiles in a lower crustal magma reservoir trapped below the Tampakan copper-gold deposit by Mio-Pliocene crustal compression in the southern Philippines*, 270 pp., PGC Publishing, Adelaide.

Rosenbaum, G., G. S. Lister, and C. Duboz (2002), Relative motions of Africa, Iberia and Europe during Alpine orogeny, *Tectonophysics*, 359(1-2), 117-129, doi: [dx.doi.org/10.1016/S0040-1951\(02\)00442-0](http://dx.doi.org/10.1016/S0040-1951(02)00442-0).

Rosenbaum, G., M. Gasparon, F. P. Lucente, A. Peccerillo, and M. S. Miller (2008), Kinematics of slab tear faults during subduction segmentation and implications for Italian magmatism, *Tectonics*, 27(2), 16, doi: 10.1029/2007tc002143.

Rosenbaum, G., D. Giles, M. Saxon, P. G. Betts, R. F. Weinberg, and C. Duboz (2005), Subduction of the Nazca Ridge and the Inca Plateau: Insights into the formation of ore deposits in Peru, *Earth Planet. Sci. Lett.*, 239(1-2), 18-32, doi: 10.1016/j.epsl.2005.08.003.

Săndulescu, M. (1984), *Geotectonica României*, 350 p pp., Editura Tehnică, Bucharest.

Săndulescu, M. (1994), Overview on Romanian Geology. 2. Alcapa Congress Field Guidebook, *Romanian Journal of Tectonics and Regional Geology*, 75(Suppl. 2), 3-15.

Sawkins, F. J. (1972), Sulfide Ore Deposits in Relation to Plate Tectonics, *The Journal of Geology*, 80(4), 377-397.

Schefer, S., V. Cvetković, B. Fügenschuh, A. Kounov, M. Ovtcharova, U. Schaltegger, and S. Schmid (2010), Cenozoic granitoids in the Dinarides of southern Serbia: age of intrusion, isotope geochemistry, exhumation history and significance for the geodynamic evolution of the Balkan Peninsula, *Int. J. Earth Sci.*, 1-26, doi: 10.1007/s00531-010-0599-x.

Schmid, S. M., T. Berza, V. Diaconescu, N. Froitzheim, and B. Fügenschuh (1998), Orogen-parallel extension in the Southern Carpathians, *Tectonophysics*, 297(1-4), 209-228, doi: 10.1016/s0040-1951(98)00169-3.

Schmid, S. M., D. Bernoulli, B. Fügenschuh, L. Matenco, S. Schefer, R. Schuster, M. Tischler, and K. Ustaszewski (2008), The Alpine-Carpathian-Dinaridic orogenic system: correlation and evolution of tectonic units, *Swiss Journal of Geosciences*, 101(1), 139-183, doi: 10.1007/s00015-008-1247-3.

Schmid, S. M., D. Bernoulli, B. Fügenschuh, A. Kounov, R. Oberhänsli, S. Schefer, D. J. J. van Hinsbergen, and K. Ustaszewski (2011), Similarities and differences between Alps Carpathians, Dinarides-Hellenides and Anatolides-Taurides, in *AGU Fall Meeting*, edited, San Francisco.

Schuller, V., W. Frisch, M. Danisik, I. Dunkl, and M. C. Melinte (2009), Upper Cretaceous Gosau deposits of the Apuseni Mountains (Romania) - Similarities and differences to the Eastern Alps, *Austrian Journal of Earth Sciences*, 102(1).

Seghedi, I., and H. Downes (2011), Geochemistry and tectonic development of Cenozoic magmatism in the Carpathian-Pannonian region, *Gondwana Research*, 20(4), 655-672, doi: 10.1016/j.gr.2011.06.009.

Seghedi, I., I. Balintoni, and A. Szakács (1998), Interplay of tectonics and neogene post-collisional magmatism in the intracarpathian region, *Lithos*, 45(1-4), 483-497, doi: 10.1016/s0024-4937(98)00046-2.

Sillitoe, R. H. (1972), A Plate Tectonic Model for the Origin of Porphyry Copper Deposits, *Econ. Geol.*, 67(2), 184-197, doi: 10.2113/gsecongeo.67.2.184.

Sillitoe, R. H. (1997), Characteristics and controls of the largest porphyry copper-gold and epithermal gold deposits in the circum-Pacific region, *Australian Journal of Earth Sciences*, 44(3), 373-388, doi: 10.1080/08120099708728318.

Sillitoe, R. H. (2010), Porphyry Copper Systems, *Econ. Geol.*, 105(1), 3-41.

Sillitoe, R. H., and J. Perelló (2005), Andean copper province: Tectonomagmatic settings, deposit types, metallogeny, exploration, and discovery, *Econ. Geol.*, 100th Anniversary Volume, 845-890.

Soldatos, T., A. Koroneos, B. K. Kamenov, I. Peytcheva, A. von Quadt, G. Christofides, X. Zheng, and H. Sang (2008), New U-Pb and Ar-Ar mineral ages for the Barutin-Buynovo-Elatia-Skaloti-Paranesti batholith (Bulgaria and Greece): Refinement of its debatable age, *Geochemistry, Mineralogy and Petrology*, 46, 85-102.

Solomon, M. (1990), Subduction, arc reversal, and the origin of porphyry copper-gold deposits in island arcs, *Geology*, 18(7), 630-633, doi: 10.1130/0091-7613(1990)018<0630:sarato>2.3.co;2.

Sosson, M., et al. (2010), Subductions, obduction and collision in the Lesser Caucasus (Armenia, Azerbaijan, Georgia), new insights, *Geological Society, London, Special Publications*, 340(1), 329-352, doi: 10.1144/sp340.14.

Stampfli, G. M., and G. Borel (2004), *The TRANSMED Transects in Space and Time: Constraints on the Paleotectonic Evolution of the Mediterranean Domain*, Springer, Berlin Heidelberg.

Stoykov, S., I. Peytcheva, A. von Quadt, R. Moritz, M. Frank, and D. Fontignie (2004), Timing and magma evolution of the Chelopech volcanic complex (Bulgaria), *Schweiz. Mineral. Petrogr. Mitt.*, 84(1-2), 101-117.

Stracke, A., A. W. Hofmann, and S. R. Hart (2005), FOZO, HIMU, and the rest of the mantle zoo, *Geochemistry Geophysics Geosystems*, 6, doi: Q0500710.1029/2004gc000824.

Stuart, C. J., M. Nemcok, D. Vangelov, E. R. Higgins, C. Welker, and D. P. Meaux (2011), Structural and depositional evolution of the East Balkan thrust belt, Bulgaria, *Aapg Bulletin*, 95(4), 649-673, doi: 10.1306/08181008061.

Sun, S.-s., and W. F. McDonough (1989), Chemical and isotopic systematics of oceanic basalts: implications for mantle composition and processes, *Geological Society, London, Special Publications*, 42(1), 313-345, doi: 10.1144/gsl.sp.1989.042.01.19.

Thirlwall, M. F., A. M. Graham, R. J. Arculus, R. S. Harmon, and C. G. Macpherson (1996), Resolution of the effects of crustal assimilation, sediment subduction, and fluid transport in island arc magmas: Pb-Sr-Nd-O isotope geochemistry of Grenada, Lesser Antilles, *Geochim. Cosmochim. Acta*, 60(23), 4785-4810, doi: 10.1016/s0016-7037(96)00272-4.

Tosdal, R., and J. Richards (2001), Magmatic and structural controls on the development of porphyry Cu±Mo±Au deposits, *Reviews in Economic Geology*, 14, 157-181.

Trumbull, R., U. Riller, O. Oncken, E. Scheuber, K. Munier, and F. Hongn (2006), The Time-Space Distribution of Cenozoic Volcanism in the South-Central Andes: a New Data Compilation and Some Tectonic Implications, in *The Andes*, edited by O. Oncken, G. Chong, G. Franz, P. Giese, H.-J. Götze, V. Ramos, M. Strecker and P. Wigger, pp. 29-43, Springer Berlin Heidelberg.

Turpaud, P., and T. Reischmann (2010), Characterisation of igneous terranes by zircon dating: implications for UHP occurrences and suture identification in the Central Rhodope, northern Greece, *Int. J. Earth Sci.*, 99(3), 567-591, doi: 10.1007/s00531-008-0409-x.

Ustaszewski, K., S. M. Schmid, B. Fügenschuh, M. Tischler, E. Kissling, and W. Spakman (2008), A map-view restoration of the Alpine-Carpathian-Dinaridic system for the Early Miocene, *Swiss Journal of Geosciences*, 101(0), 273-294, doi: 10.1007/s00015-008-1288-7.

Ustaszewski, K., A. Kounov, S. M. Schmid, U. Schaltegger, E. Krenn, W. Frank, and B. Fügenschuh (2010), Evolution of the Adria-Europe plate boundary in the northern Dinarides: From continent-continent collision to back-arc extension, *Tectonics*, 29, doi: 10.1029/2010tc002668.

van Hinsbergen, D. J. J., and S. M. Schmid (2012), Map view restoration of Aegean-West Anatolian accretion and extension since the Eocene, *Tectonics*, 31, doi: 10.1029/2012tc003132.

van Hinsbergen, D. J. J., E. Hafkenscheid, W. Spakman, J. E. Meulenkamp, and R. Wortel (2005), Nappe stacking resulting from subduction of oceanic and continental lithosphere below Greece, *Geology*, 33(4), 325-328, doi: 10.1130/g20878.1.

van Hinsbergen, D. J. J., G. Dupont-Nivet, R. Nakov, K. Oud, and C. Panaiotu (2008), No significant post-Eocene rotation of the Moesian Platform and Rhodope (Bulgaria): Implications for the kinematic evolution of the Carpathian and Aegean arcs, *Earth Planet. Sci. Lett.*, 273(3-4), 345-358, doi: 10.1016/j.epsl.2008.06.051.

Velichkova, S. H., R. Handler, F. Neubauer, and Z. Ivanov (2004), Variscan to Alpine tectonothermal evolution of the Central Srednogorie unit, Bulgaria: constraints from Ar-40/Ar-39 analysis, *Schweiz. Mineral. Petrogr. Mitt.*, 84(1-2), 133-151.

Vlad, Ş. N. (1997), Calcic skarns and transversal zoning in the Banat mountains, Romania: indicators of an Andean-type setting, *Miner. Depos.*, 32(5), 446-451, doi: 10.1007/s001260050113.

von Huene, R., and C. R. Ranero (2009), Neogene collision and deformation of convergent margins along the backbone of the Americas, *Geol. Soc. Am. Mem.*, 204, 67-83, doi: 10.1130/2009.1204(03).

von Quadt, A., and I. Peytcheva (2005), The southern extension of the Srednogorie type Upper Cretaceous magmatism in Rila-Western Rhodopes: Constraints from isotope geochronological and geochemical data, paper presented at 80 years Bulgarian Geological Society, Bulgarian Geological Society, Sofia, Bulgaria.

von Quadt, A., R. Moritz, I. Peytcheva, and C. A. Heinrich (2005), 3: Geochronology and geodynamics of Late Cretaceous magmatism and Cu-Au mineralization in the Panagyurishte region of the Apuseni-Banat-Timok-Srednogorie belt, Bulgaria, *Ore Geology Reviews*, 27(1-4), 95-126, doi: DOI: 10.1016/j.oregeorev.2005.07.024.

von Quadt, A., I. Peytcheva, B. Kamenov, L. Fanger, C. A. Heinrich, and M. Frank (2002), The Elatsite porphyry copper deposit in the Panagyurishte ore district, Srednogorie zone, Bulgaria: U-Pb zircon geochronology and isotope-geochemical investigations of magmatism and ore genesis, in *Timing and Location of Major Ore Deposits in an Evolving Orogen*, edited by D. J. Blundell, F. Neubauer and A. von Quadt, pp. 119-135.

von Quadt, A., M. Erni, K. Martinek, M. Moll, I. Peytcheva, and C. A. Heinrich (2011), Zircon crystallization and the lifetimes of ore-forming magmatic-hydrothermal systems, *Geology*, 39(8), 731-734, doi: 10.1130/g31966.1.

Willingshofer, E., F. Neubauer, and S. Cloetingh (1999), The significance of Gosau-type basins for the late cretaceous tectonic history of the Alpine-Carpathian belt, *Physics and Chemistry of the Earth, Part A: Solid Earth and Geodesy*, 24(8), 687-695, doi: 10.1016/s1464-1895(99)00100-3.

Willingshofer, E., P. Andriessen, S. Cloetingh, and F. Neubauer (2001), Detrital fission track thermochronology of Upper Cretaceous syn-orogenic sediments in the South Carpathians (Romania): inferences on the tectonic evolution of a collisional hinterland, *Basin Research*, 13(4), 379-395, doi: 10.1046/j.0950-091x.2001.00156.x.

Workman, R. K., and S. R. Hart (2005), Major and trace element composition of the depleted MORB mantle (DMM), *Earth Planet. Sci. Lett.*, 231(1–2), 53-72, doi: 10.1016/j.epsl.2004.12.005.

Wörner, G., S. Moorbath, and R. S. Harmon (1992), Andean Cenozoic volcanic centers reflect basement isotopic domains, *Geology*, 20(12), 1103-1106, doi: 10.1130/0091-7613(1992)020<1103:acvcrb>2.3.co;2.

Wortel, M. J. R., and W. Spakman (2000), Geophysics - Subduction and slab detachment in the Mediterranean-Carpathian region, *Science*, 290(5498), 1910-1917.

Yosifov, D., and V. Pchelarov (1977), A scheme of the thickness of the Earth's crust in the Balkan Peninsula and some features of its structures, *Geologica Balcanica*, 7, 7-22.

Zimmerman, A., H. Stein, J. Hannah, D. Koželj, K. Bogdanov, and T. Berza (2008), Tectonic configuration of the Apuseni–Banat—Timok–Srednogorie belt, Balkans-South Carpathians, constrained by high precision Re–Os molybdenite ages, *Miner. Depos.*, 43(1), 1-21, doi: 10.1007/s00126-007-0149-z.